PHASE EVOLUTION, POWDER MORPHOLOGY AND PHOTOLUMINESCENCE BEHAVIOR OF EUROPIUM ION DOPED ZINC OXIDE AND ZINC OXIDE-ZINC BORATE POWDERS

Rajib Lochan Rautaray

Department of Ceramic Engineering
National Institute of Technology Rourkela

PHASE EVOLUTION, POWDER MORPHOLOGY AND PHOTOLUMINESCENCE BEHAVIOR OF EUROPIUM ION DOPED ZINC OXIDE AND ZINC OXIDE-ZINC BORATE POWDERS

Thesis submitted in partial fulfillment

of the requirements of the degree of

Dual Degree (B. Tech & M. Tech)

in

Ceramic Engineering

by

Rajib Lochan Rautaray

(Roll Number: 711CR1107)

based on research carried out

under the supervision of

Prof. Bibhuti B. Nayak

Department of Ceramic Engineering
National Institute of Technology Rourkela

May 2016

Department of Ceramic Engineering
National Institute of Technology Rourkela

Prof. Bibhuti Bhusan Nayak (Ph.D., IIT Bombay)

Associate Professor and HOD
Department of Ceramic Engineering
National Institute of Technology Rourkela
PIN: 769 008, INDIA
Email: bbnayak@nitrkl.ac.in; bibhutib@gmail.com
Phone: 0661-246-2209/2201 (O); +91-9861422166 (M)

Date:

Supervisor's Certificate

This is to certify that the work presented in the thesis entitled "Phase evolution, powder morphology and photoluminescence behavior of europium ion doped zinc oxide and zinc oxide-zinc borate powders", submitted by Rajib Lochan Rautaray, Roll Number 711CR1107, is a record of original research carried out by him under my supervision and guidance in partial fulfillment of the requirements of the degree of *Dual Degree (B. Tech and M. Tech)* in *Department of Ceramic Engineering*. Neither this thesis nor any part of it has been submitted earlier for any degree or diploma to any institute or university in India or abroad.

_____

Bibhuti Bhusan Nayak

Declaration

I, Rajib Lochan Rautaray, Roll Number 711CR1107, hereby declare that, this Dual Degree (B. Tech & M. Tech) project thesis work entitled "Phase evolution, powder morphology and photoluminescence behavior of europium ion doped zinc oxide and zinc oxide-zinc borate powders" presents the original work carried out as a Dual degree (B. Tech and M. Tech) student of NIT Rourkela.

To the best of my knowledge, the matter embodied in the thesis has not been submitted to any other university/institute for the award of any Degree or Diploma.

Date:

NIT Rourkela Rajib Lochan Rautaray

Acknowledgments

I would like to take this auspicious moment to express my sincere gratitude, and indebtedness from the core of my heart to Prof. Bibhuti B. Nayak for assigning me this project, for his continuous guidance, valuable suggestions and strict criticism without which completion of my project work would not have been possible at all.

I wish to express my appreciation to all the Professors of Department of Ceramic Engineering for their constant support and inspiring words.

This gratitude will be left with unfilled unless I express my deep thankfulness to Subham Didi, who has been the companion as well as the captain of my ship through this stormy voyage of this project throughout the year.

I want to thank all the lab in-charges especially Mr. P.K. Mohanty sir, Arvind sir for their help in lab works that were an important part of this project.

My genuine thanks to Jayrao Bhai and all the research scholars, M. Tech students and juniors for their support, valuable advises and guidelines and help in times of need and my dual degree friends for supporting me and being the pillar for motivation throughout the graduation.

Last but not the least I thank God, for giving me the courage and blessings for completion of this work.

I would like to dedicate this complete work to my Bapa ,Maa, Bhai, and especially my Dei whose continuous inspiring word keeps me motivated & ignites my appetite for the research.

Date:

NIT Rourkela

Rajib Lochan Rautaray

Roll No: 711CR1107

Abstract

Phosphor materials have performed as a potential candidate in the field of lighting applications. So, in this present work zinc oxide (ZnO) and mixture of ZnO and zinc borate powders were synthesized via borohydride method using sodium borohydride ($NaBH_4$) as a precipitating agent. Thermal behavior of as-synthesized powders was characterized using DSC-TG. In addition, the experimental condition was optimized by varying the parameters such as number of washing and calcination temperature to produce pure ZnO and mixture of ZnO and zinc borate. Moreover, effect of number of washing and precursor salts (such as zinc acetate and zinc chloride) on the phase evolution of ZnO or zinc borate during calcination process was studied in detail. The borohydride derived ZnO-based materials have been used as a host material, and it was doped with 10 mol % trivalent europium (Eu^{+3}) ions for further studying the structure, microstructure and photoluminescence behavior. Structure and powder morphology was studied using XRD and FESEM, respectively. Optical properties of borohydride derived Eu-doped ZnO based powders was studied using UV-vis spectroscopy and photoluminescence spectroscopy. The photoluminescence behavior of Eu-doped pure ZnO as well as Eu-doped ZnO-zinc borate sample was analyzed at an excitation wavelengths of 254 nm, 365nm, and 390 nm. The present research work suggests the potential of borohydride method for the development of Eu-doped pure ZnO and Eu-doped ZnO-zinc borate powders and further proposes the potential of these materials in the field of lighting applications.

Keywords: Zinc oxide; Zinc Borate; Sodium borohydride; Photoluminescence; Powder morphology.

Table of Contents

List of Figures

List of Tables

List of Abbreviations

Index No.	Abbreviations	Full Form
1	XRD	X Ray Diffraction
2	FESEM	Field Emission Scanning Electron Microscope
3	DSC	Differential Scanning Calorimetry
4	TGA	Thermal Gravimetry Analysis
5	UV-Vis	Ultra Violet – Visible
6	PL	Photoluminescence
7	GPa	Giga Pascal
8	MeV	Mega electronVolt
9	nm	Nanometer
10	RF	Radio Frequency
11	ml	Mili Liter

List of Symbols

Index No.	Symbol	Symbol Name
1	^{0}	Degree
2	θ	Theta
3	λ	Lambda
4	c	Speed of Light
5	h	Plank's Constant
6	α	Alpha
7	β	Beta
8	ν	Nu
9	Å	Angstrom

Chapter 1

INTRODUCTION

Looking at the history of few centuries, the revolution that was brought in the field of science and technology has given a boost for the creation of ideas and innovation for the betterment of mankind. Energy sector being the most demanding need of the era, all attentions have been focused in this area to make it never-ending. There has been a huge growth in the field of material technology and material science owing to its demand in the energy sector. Depending on the properties, various materials are manufactured according to its requirements. The huge development in the field of lighting devices such as LEDs (Light Emitting Diodes) and opto-electronic application has brought the energy sector to a new level fulfilling the demand of energy deficit society. This has been possible only due to the successful operation of the luminescent materials which require very subtle energy as compared to the conventional lighting materials such as tungsten. The tungsten in incandescent bulb work with the operation of light generation from the heat generated. However, the LEDs work with the principle of luminescence for generation of light. Luminescence is the phenomenon that takes place with certain kind of substances which emit light when absorbing various energies without the generation of heat. The luminescence is characterized by the wavelength of the light emitted which determines the color produced. In order to anlyze the luminescence behavior, Photoluminescence spectroscopy was used. Photoluminescence spectroscopy is the contact-less, non-destructive process of probing the electronic structure of the material. Here light is directed onto the sample, where it is absorbed and imparts excess energy into the material in a process called photo-excitation [1]. This excess energy is dissipated through the emission of light or luminescence. So in case of photo-excitation this is call photo-luminescence. These photo excited electrons can move within the material into permissible excited states and when these excited electrons return to the equilibrium state by releasing energy in the form of light (radiation). The energy of light emitted depends on the difference between the energy levels of the excited state and the ground state. This photo-luminescence can be categorized into two types such as fluorescence and phosphorescence, depending on the mechanism of the process.[2] Fluorescence is the emission of light by a substance that has absorbed light or other electromagnetic radiation. It is a form of photoluminescence. In most cases, the emitted light has a longer wavelength, and therefore lower energy, than the absorbed radiation. Then due to vibrational relaxation the electrons come back to the lowest energy state of the excited band. Phosphorescence is a specific type of photoluminescence related to fluorescence. As discussed in the previous section about fluorescence, as it emits light quickly after relaxation but, aophosphorescent material does not instantly re-emit the

radiation it absorbs. In this present work, luminescence properties of europium doped zinc oxide and europium doped zinc oxide-zinc borate sample was studied. Zinc oxide is one of the most efficient semiconductors considering its wide range of properties.[3] Crystalline zinc oxide is thermochromic, changing from white to yellow when heated and in air reverting to white on cooling. As reported from various literature the band gap of ZnO films mostly depends on the carrier concentration and is found to be 3.37ev on the basis of the carrier concentration [4]. Zinc oxide can be used in various applications such as

1. ZnO nanoparticles are used in cosmetic applications as gas sensors, biosensors, and photo-catalytic applications. Due to its UV blocking properties the sun rays is unable to penetrate through it.
2. ZnO nanoparticles are also used in solar cells (dye-sensitized), photoluminescence and sensor application.
3. It also has an extensive utilization in the field of bio-applications. Due to its biocompatibility and water solubility, it is preferred in applications for drug delivery system and nanomedicines.[5]

Rare earth doped zinc oxide can be used as a luminescence materials and was discussed in the literature section.

Chapter 2

LITERATURE REVIEW

In this section, effort has been made to observe and review the previous work done by the researchers in the field of luminescence of undoped ZnO, Eu^{+3}-doped ZnO, and phosphor borate material.

Considering the ZnO material which is used as semiconducting material in wide applications of optical applications and the opto-electronic applications as well. The most conventional and time effective way of production is found to be the solid-state route. Hou *et. al* [6] found a very simple synthesis method preparation of ZnO nanoparticles by solid state reaction at room temperature. They used $ZnCl_2$ and RTILs and mixed thoroughly. Again it was mixed with NaOH followed by washing and centrifuging which was dried at 60 ^{o}C for 10hrs. It produced a nano-rod structure with length 80nm – 100nm with a diameter of 1 nm. The PL intensity curve showed a peak at the position at 536nm corresponding to the green region which is due to the structural defects. But Mishra *et. al* followed the same procedure of solid state method by mixing zinc sulfate heptahydrate ($ZnSO_4.7H_2O$) and sodium hydroxide (NaOH) with a molar ratio of 1:4 and ground vigourously [7]. It was followed by mixing 0.04mol of NaOH, and the sample was washed, filtered and dried at 80 ^{o}C. This sample was annealed at 450 ^{o}C and 650 ^{o}C. This process showed smaller particle size than the previous one and in the PL intensity curve it showed a number of intense peaks in Violet, Blue, Green-blue region which can be used for the production of light with a combination of colors. Though luminescence is observed in the solid-state route but the control over the particle size is very challenging and high temperature is required in this process which makes us look for other better routes for synthesis.

In many synthesis processes the combustion route is adopted due to its easy method, time-saving with the ability to produce powder in a larger amount. SOWRI BABU [8] *et. al* used porous structure of ZnO nanopowders using a very cheap and efficient method of self-propagating combustion reaction. It was prepared by taking Zinc Nitrate solution and dissolving it in an ethanol solution in heated conditions. After formation of the clear solution, its temperature was increased up to 80^{0}C and kept there until the foam formation takes place by combustion reaction. It was calcined at 300 ^{o}C and 500 ^{o}C which showed amorphous powder at lower temperature but gradually became crystalline at 500 ^{o} C. The room-temperature PL analysis showed peaks starting from the violet region to green region at nearly 437nm, 466nm, 492nm and 531nm whose intensity increases for the higher temperature calcined sample.But Tarwal *et. al* [9] followed a very modest way of

combustion where they prepared an aqueous solution of zinc nitrate ($Zn(NH_3)_2 \cdot 6H_2O$) precursor and used glycine ($C_2H_5NO_2$).The solution heated at 100 ^oC on hot-plate and after several hours combustion takes place producing fine powders. It produced a perfectly crystalline structure with the crystallite size (25nm) were much finer than the previous process. Here the Pl emission shows an intense peak in the UV region at 398nm and relatively less intense peak in near green region of 471nm. However, the particle size and particle morphology were found to be non-uniform in this route and production of desired properties makes needs a large number of optimizations which makes it less preferred than the process producing ample amount of nanostructures.

In many pyrolysis water is used as a better solvent of metal-ionic compound under high pressure and high temperature producing fine metal powders.[10]. This process provides better control over the particle size and shape and lower calcination temperature is required as well. Fan *et. al* [11] synthesized ZnO nano rods by the same hydrothermal process where the appropriate amount of Zinc nitrate and ammonium carbonate were mixed proper ratio at a constant pH of 8. Then the solution was taken in an autoclave unit and kept at a temperature of 180 ^oC for 20hrs. The product powder was centrifuged and dried for 8-9 hrs. This produced nano rods with an average length of 300nm. Its PL analysis at an excitation wavelength of 325nm showed an intense peak in the UV region at 387nm and a less intense but broad peak at 600nm due to the recombination emission of interstitial oxygen and0conduction band. But Kumari *et. al* followed the same process but in a different approach. [12] They used Zn plate both as source and the substrate to be deposited. After perfectly cleaning the plate it was taken in the autoclave with 80vol% filled with aqueous ammonia solution. It was kept at 150 ^oC for 2 hrs which produced ZnO powder deposited on the plate. After characterization, it was observed to produce perfectly crystalline phase of ZnO with crystallite size of 30nm. Its PL intensity curve showed peaks in the UV region and the near green region owing to the intrinsic defects. Irrespective of these properties this route can be complex due to its potential for corrosion and higher synthesis conditions required.

That is why we prefer for a route which producing nanostructures which give excellent properties due to the high surface to volume ratio, high chemical, and photo-chemical stability, uniformity in pore size, surface selectivity and high surface chemistry [13]. Hence, wet chemical route is preferred over the other ones. Taunk *et. al* [14] used a proper molar ratio Zinc Chloride with an aqueous solution sodium hydroxide followed by

appropriate amount of TEA solution being added to it. The solution was kept for 24h and then washed for 8 times and dried it. The 190 ^{o} C calcined powder was characterized by XRD to confirm the presence of crystalline phase of ZnO. The particle produced, comes within the size range of 7nm-21nm confirmed by TEM. The PL spectra for the excitation in blue region of 407nm and a broad peak at 487nm owing to the radiative recombination of a photo-generated hole with an electron. But the use of a reducing agent has a very constructive contribution for production of luminescent ZnO particles. Shit *et. al* [15] followed a route where they prepared an aqueous solution of Zinc Acetate Dihydrate, which was mixed into another solution prepared by mixing TEA into the solution of Benzene-1,3,5-tricarboxylic acid, maintaining the proper molar ratio. The solution was kept for precipitation and then washed several times followed by calcination at 550 ^{o} C. It was observed to produce nano-spheres of ZnO with average diameter of 100nm. Lookin at the PL spectra of the nano-powder with an excitation wavelength of 377nm it produced strong emission peak at 387nm in the UV region owing to the defect-free crystal of ZnO along with less intense broader peaks in the blue region. These better properties make wet chemical precipitation route more suitable for the formation of ZnO nanopowders.

For doping of Eu^{+3} ion onto the zinc oxide matrix many routes were studied that confirmed the doping of europium with a positive effect towards the luminescence of the ZnO powder.

Following the conventional route of solution-combustion method Lopez at. al [16] used Zinc nitrate hexahydrated0($Zn(NO_3)_2 \cdot 6H_2O$) as an oxidizer, urea (H_2NCONH_2) as fuel, and Europium chloride ($EuCl_3$) as a dopant. The wt% of Eu ion was varied from 1% to 10%. Appropriate amount of raw material were taken and an aqueous solution of it were prepared which was kept on the hot-plate at 500 ^{o} C and after an incandescent flame the powder was developed and it was calcined at 900 ^{o} C. Comparing the lattice parameters of both doped and undoped ZnO the lattice parameters of Eu-doped ZnO increased due to the increased lattice distortion. The crystallite size decreased due to doping from 41nm to 18nm. Considering the photoluminescence of the doped sample i.e. excited at 270nm in the UV range with a broad green emission in the 516nm and an intense peak in the red region 579nm to 640nm due to intra 4f transition of $^{5}D_0 \rightarrow {}^{7}F_j$ (j = 0, 1, 2, 3). The peak intensities increase with increase in doping content. However, Pessoni *et. al* [17] used the same route with using Europium nitrate, zinc nitrate, and urea as fuel in proper molar ratio. The continuous heating at 350 ^{o} C in hot plate produced combusted powder after few hours. The XRD analysis shows the Eu_2O_3 along with major matrix phase of ZnO powder. Though the PL curve shows

peaks at same positions as the powder prepared by the previous route, however, the ratio of the peak intensities was less as compared to the other one. This confirms the symmetricity of the structure of this powder. But for the production of Eu-doped ZnO using a conventional and easy process the wet chemical precipitation method is adopted.

Even if in many cases for the production of uniformly distributed nanoparticles the reverse micelle method is approached. Ishizumi *et. al* [18] approached the reverse micelle method for the formation of Eu—doped ZnO nanocrystals using a surfactant in hydrophobic solvent. They used cetyl0trimethyl ammonium bromide (CTAB), butanol, and octane as surfactant, co-surfactant, and hydrophobic solvent, respectively. For the pyrolysis of the $Zn(OH)_2$: Eu NCs, Zinc acetate (dihydrate) ,Europium acetate (dihydrate), and aqueous ammonia were used. Two mol% of Eu ion was taken. The hydroxides were dehydrated at 200 ^{o}C for 10h to obtain the nanocrystals. It produced very fine-sized quantum nano-crystals with diameter nearly 10nm. It showed the PL intensity peak at a position of 3.36eV due to intrinsic defects for ZnO host and intense peaks in the red region from 1.7eV to 2.1eV due to the 4f transition taking place in europium. This process is very efficient for producing the Eu-doped ZnO. However Shahroosvand *et. al* [19] followed a solution based precipitation synthesis route for doping of Eu^{+3} ion into ZnO where they used Zinc acetate/zinc oxide as the zinc source, Europium nitrate as the doping agent with Sodium Borohydride ($NaBH_4$) as the reducing agent. They were added in aqueous form in different sequence to observe the difference in the powder formed. Irrespective of doping there is no peak for europium in the XRD. Considering the PL intensity curve, though the concentration of the Eu^{+3} ion used is same, but the peak intensities are different as due to different processes approached different amount of Eu ions goes into the structure. But the peak position are same as of the previous one showing small green peak due to the intrinsic defects and major red luminescence due to 4f transitions.

The wet chemical precipitation route is found to be very operative for doping of materials. The use of a precipitating agent has a tremendous effect on the successful synthesis of powder with fine particle size. Srivastava et al. [20] adopted the wet chemical precipitation route for the synthesis of YBO_3: Eu^{+3} nano phosphor material.

They used sodium borohydride ($NaBH_4$) as the precipitating agent which helped in the formation of the desired phase with nearly spherical dumbbell-shaped particles with a size in the range of 200nm – 700 nm. The emission intensities showed peaks at the respective positions for europium ion.

There has been a vast research in the field of luminescence of the borate system. It can act as an enhancer of the luminescence of the material by controlling the composition. Ivankov *et. al* [21] observed the absorption and fluorescence of the zinc borate glass. They used ZnO and B_2O_3 in different molar ratio and after mixing the oxides they melted it at 1200 ^{o}C for 10 minutes and quenched by taking a drop of melt into two brass plates and pressing them to produce glass disk. Observing the fluorescence with an excitation wavelength 245nm shows a wide UV-blue emission in the range of 260 nm to 550nm with the intense peak positioned at 340nm. The change in composition has a significant effect as well. With the increase in ZnO content, the peak position was red shifted gradually. They considered the ZnO crystal responsible for the luminescence of the system.

Considering the successful phase evolution of the required phase this borohydride route can be used for the synthesis of ZnO and Eu-doped ZnO.

But considering the Eu-doped ZnO and the Zinc borate system, many researchers have observed the enhancement of luminescence due to borate phase. Zheng *et. al* [22] studied the photoluminescence when Eu ion was doped into zinc borate using the co-precipitation method. They used borax ($Na_2B_4O_7.10H_2O$) as the source of boron, whose aqueous solution was made. The solution of Eu_2O_3 dissolved into the nitric acid was added drop-wise to the borax solution. It was heated at 60 ^{o}C with the addition of a proper amount of Zinc sulfate. After complete precipitation, it was washed and then a white precipitate of $Zn_3B_{10}O_{18}\cdot 4H_2O$: Eu^{3+} was obtained which was further calcined. It showed the characteristic PL intensity behavior as that of Eu ion, but the peak intensity decreased after 5mol% which was caused by concentration quenching. It was confirmed that the intensity in the red region (612nm) was enhanced by the presence of Zinc borate system.

However, there has been a vast research in the field of luminescence of undoped Zinc Borate. Terol *et. al* [23]observed the luminescence of anhydrous zinc borate as a host crystal. They used boric acid (H_3BO_3) as the source of B_2O_3 which was obtained after melting boric acid at a temperature 1100 ^{o}C. It was mixed with appropriate amount of Zinc oxide, followed by quenching to form the glass. It was dissolved with HCl to get cubic Zinc borate phase. For composition with ZnO content 61% it shows violet emission at 2537 Å emission whereas for 70% composition it shows emission in the yellow region. They observed the high strength of BO_4 tetrahedra while increasing the Zn content in the lattice might fragment the 3D lattice which gives rise to luminescence.

2.1Objectives:-

- To find out a suitable reagent which is a source of boron and also help for precipitating the zinc-salts and further produces zinc oxide as well as zinc-borate based materials.

- Study the phase evolution of zinc oxide and zinc borate as well as powder morphology of zinc oxide and zinc borate by varying washing time, changing precursor and calcination temperature.

- To develop Eu^{3+}-doped zinc oxide and Eu^{3+}-doped zinc oxide-zinc borate based materials.

- To study the photoluminescence behavior of the Eu^{3+}-doped zinc oxide and Eu^{3+}-doped zinc oxide-zinc borate based materials.

Chapter 3

EXPERIMENTAL

3.1 Synthesis of Zinc Oxide

The synthesis was done by the co-precipitation method. The initial batch was prepared for the un-doped Zinc oxide (ZnO). For this synthesis, the chemicals required were

- Zinc Chloride ($ZnCl_2.H_2O$) (Sigma Aldrich)
- Zinc Acetate ($Zn(CH_3COO)_2).(H_2O)_2$
- Sodium Borohydride ($NaBH_4$)

The batch was prepared by taking initially 1Molar of Zinc Chloride dissolved in a beaker with DI water by continuous stirring which produces a clear solution quickly. Then another solution 0.5Molar Sodium Borohydride was prepared. It was followed by gradual addition of the chloride solution from the buret drop by drop onto the $NaBH_4$ solution taken in the beaker. Then progressively its pH decreases which were initially at 10 before any addition of the acidic chloride solution. Then its pH was maintained at 10 by adding $NaBH_4$ again to it from another buret. This process continued until all the chloride solution was consumed by maintaining the 10 pH value. Then it was left for one night to settle down. Then it was washed with hot water after mixing and stirring with hot water to remove the impure phases and again it was left for settling for few hours before further washing. This process was repeated for 20 times. Then it was kept in a vacuum oven for one whole night for drying. Then the dried sample was ground and then calcined at 450^0C, 600^0C and 800^0C.

The same procedure was followed by varying the precursor and by preparing 1Molar of acetate solution.

For optimizing the process which should produce lowest amount of the impurity phase we varied the number of washings by 10, 20 and 30 as well by the above procedure and prepared three different batches to analyze.

3.2 Synthesis of Eu-doped Zinc oxide

This process required preparing a $EuCl_2$ solution which was synthesized by dissolving required amount of Europium Oxide with Hydrochloric Acid in heated conditions. This $EuCl_2$ was mixed to the above $ZnCl_2$ solution to prepare a 10mol% solution. Then for the further process, same procedure which was followed as mentioned in section 3.1.

3.3 Characterization Techniques

3.3.1 Physical Characterization

3.3.1.1 Phase Analysis

The phase analysis is done by the XRD (X-Ray Diffraction) method. Wilhem Rontgen had discovered the existence of X-Ray, and its nature was still undetermined. The wavelength of the X-Ray in the range of 0.4 Å – 0.6 Å, which was comparable to the interatomic distance of the atoms, for which diffraction becomes possible producing good results of the crystalline structure. These lattices form a series of parallel planes with its own specific d-spacing and with different orientations exist. For this diffraction to occur the X-Ray should obey the Bragg's Law According to which, the path between to X-Rays interacting with two parallel planes should be a multiple of the wavelength.

Bragg's Law: $n\lambda = 2d\sin\theta$

Where n= order of diffraction

λ= wavelength (for Copper source 1.5405 Å)

d= Inter-planar spacing

θ= Bragg's angle

Here the X-ray Diffraction performed with the help of Rigaku's Diffractometer (modelultima 4, Japan). It used copper as the source material. For the detection of diffracted X-rays, there is an electronic detector on the other side of the sample in the X-ray tube. The sample is then rotated through different Bragg's angles. The track of the angle (θ) is kept with the help of a goniometer, the detector records the detected X-rays in counts/sec and sends this data to the computer. After the complete scan of the sample, the X-ray intensity versus angle theta (2θ) is plotted. The data was analysed by using the X'pert Highscore software. This XRD data helps in determining the phases present, crystallite size, crystal structure, lattice parameters, etc. Crystallite size was determined using Scherrer's formula

3.3.1.2 Thermal Analysis

The thermal characterization consist of the DSC (Differential Scanning calorimetry) and TGA(Thermal Gravimetry Analysis) . This was done for the green powder by the NETZSCH STA (Model No 409C) instrument. The DSC technique is useful for determining the phase transitions, decomposition temperature, glass transition point, formation of products during synthesis, etc. This shows the type of the reaction whether endothermic or exothermic according to the direction of the peak. The TGA shows the weight loss corresponding to a reaction. This determines the stability of the sample throughout the temperature range. This weight loss may take place due to the evolution of surface water, crystalline water, gases from reactions. In some cases, we may even observe weight gain due to reaction with the atmosphere.

3.3.2. Microstructural Analysis

Here the microstructural analysis is done by FESEM (Field Emission Scanning Electron Microscope)(Nova Nano SEM/FEI 450) instrument. This works with an FEG (Field Emission Gun) where it is placed under a very high electric field of nearly 10^9 v/m being applied on a sharp tip of the gun (10^{-6} to 10^{-7}m). The electron beam is focused and controlled by various condenser lenses and objective lenses present in the system. When the electrons react with the sample, then the interaction causes production low energy Secondary Electrons (SE), elastically scattered Back Scattered Electrons (BSE) and electromagnetic X-Rays. The SEs produced from the surface of the sample are received by the detector which produces the image on the screen.[24]

3.3.3. Optical Characterization

3.3.3.1 UV-Vis Spectroscopy

The UV-Visible spectroscopy is the characterization to observe the absorption of the sample under light within the Ultra Violet range (200nm - 400nm) and Visible light range (400nm - 700nm). This instrument operates with the mechanism that when a visible light / UV light is passed through a prism or diffractometer, it splits the light into each wavelength. The monochromatic beam is divided into two equal intense beams one of which passes through a cuvette containing sample and the other half of the beam is passed through the cuvette,

having solvent without sample. The light passed through both of the cuvettes and the intensity of the light after passing the sample was taken as I, whereas the intensity of light passed through the reference which absorbs nearly nothing which is taken as I_0. The absorbance is calculated as $A = \log (I_0/I)$. The absorption was measured by the instrument SHIMADZU UV-2450 UV-Vis spectrophotometer.

3.3.3.2 Photoluminescence

Here the atoms of the powder were excited at different excitation wavelengths and then the emission spectra was observed in which graph was plotted between wavelength and intensity. The instrument used for the measurement of PL is HORIBA FluoroMax-4 Spectrofluorometer. [25].

Results

&

Discussions

Chapter 4

Effect of washing and calcination temperature on the phase evolution and powder morphology of zinc oxide and or zinc borate

4.1 Introduction

This chapter deals with the synthesis of zinc oxide powders via borohydride route using $NaBH_4$ using chloride precursor. In addition, the precipitated powders after the reaction were washed with three different times such as 10, 20 and 30 times with hot water. Further, these washed samples were calcined at 600 °C and 800 °C. Phase evolution was studied using XRD and powder morphology of these powders were analysed using FESEM.

4.2 Phase evolution

Phase evolution of the powders washed at three different times, were calcined at 600 °C and 800 °C in order to study the phase evolution of zinc oxide in the powder. The phase analysis of these powders was analyzed using XRD. Fig. 4.1 shows the XRD patterns of the calcined (600 °C) powder prepared by chloride precursor by varying number of washing such as 10, 20 and 30 times. All the peaks are indexed with pure zinc oxide (ZnO) as per the JCPDS file number: 79-0206. There is no indication of impurity phase in the calcined 600 °C sample. Phase pure ZnO was developed after calcination of 600 °C even after washing for 10 times. Further, the different time washed sample was calcined at 800 °C and phase analysis was performed using XRD. Fig. 4.2 shows the XRD patterns of the calcined (800 °C) powder prepared by chloride precursor by varying number of washing such as 10, 20 and 30 times. When the precipitated powders were washed for 10 times and calcined at 800 °C, a minute amount of zinc borate ($Zn_3(BO_3)_2$) (as per JCPDS file number: was evolved along with major phase of ZnO. However, when the precipitated powders were washed for more than 10 times, i.e. 20 and 30 times, only ZnO phase was developed. There was no indication of zinc borate phase even after washing for 20 or 30 times. The XRD analysis suggests that the phase evolution of zinc borate in zinc oxide matrix was dependent on the number of washing. Based on the XRD analysis, the number of washing was fixed for more than 20 times.

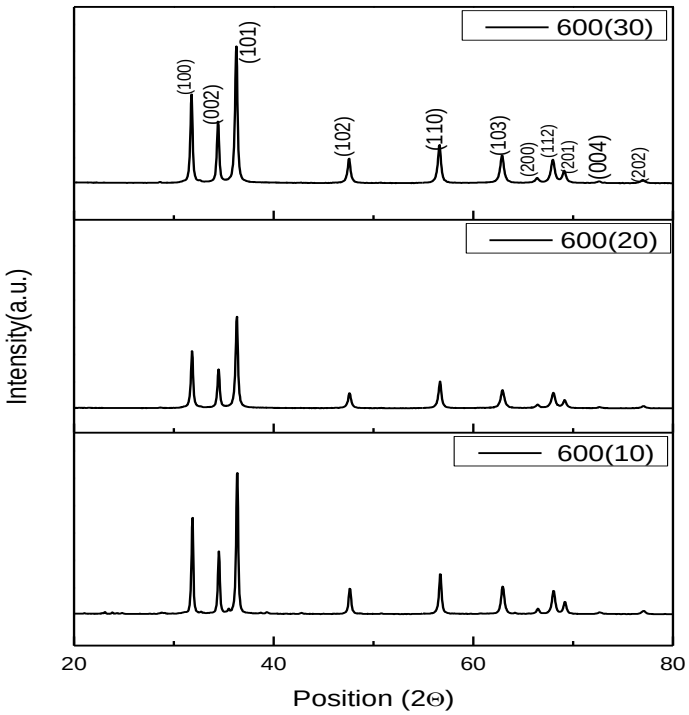

Figure 4.1: XRD patterns of the calcined (600 °C) powder prepared by chloride precursor by varying number of washing such as 10, 20 and 30 times.

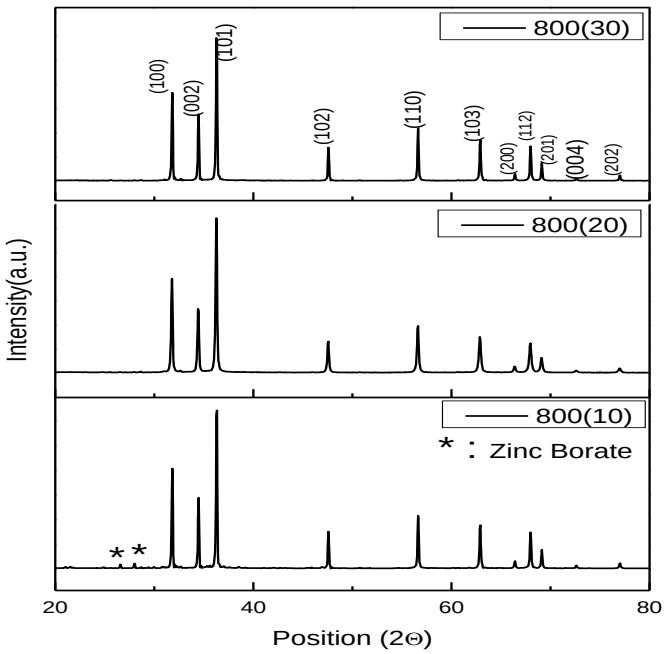

Figure 4.2: XRD patterns of the calcined (800 °C) powder prepared by chloride precursor by varying number of washing such as 10, 20 and 30 times.

4.3 Powder morphology

In order to understand the powder morphology of these powders, FESEM was performed on different washed samples, calcined at 600 °C and 800 °C. Fig. 4.3 (a), (b) and (c) shows FESEM micrograph of calcined (600 °C) zinc oxide powder prepared using $NaBH_4$ and washed for 10 times, 20 times and 30 times, respectively. When the powders were washed for 10 times and calcined at 600 °C, the powder morphology show agglomerated in nature. The particles are in the range of 500 nm to 1µm. However, the powders washed for more than 20 or 30 times, the powder morphology changes to smaller in size, but agglomerated in nature. In addition, the agglomerated particles consist of finer particles having size in the range between 30 nm to 100 nm, as compared to the samples washed for 10 times.

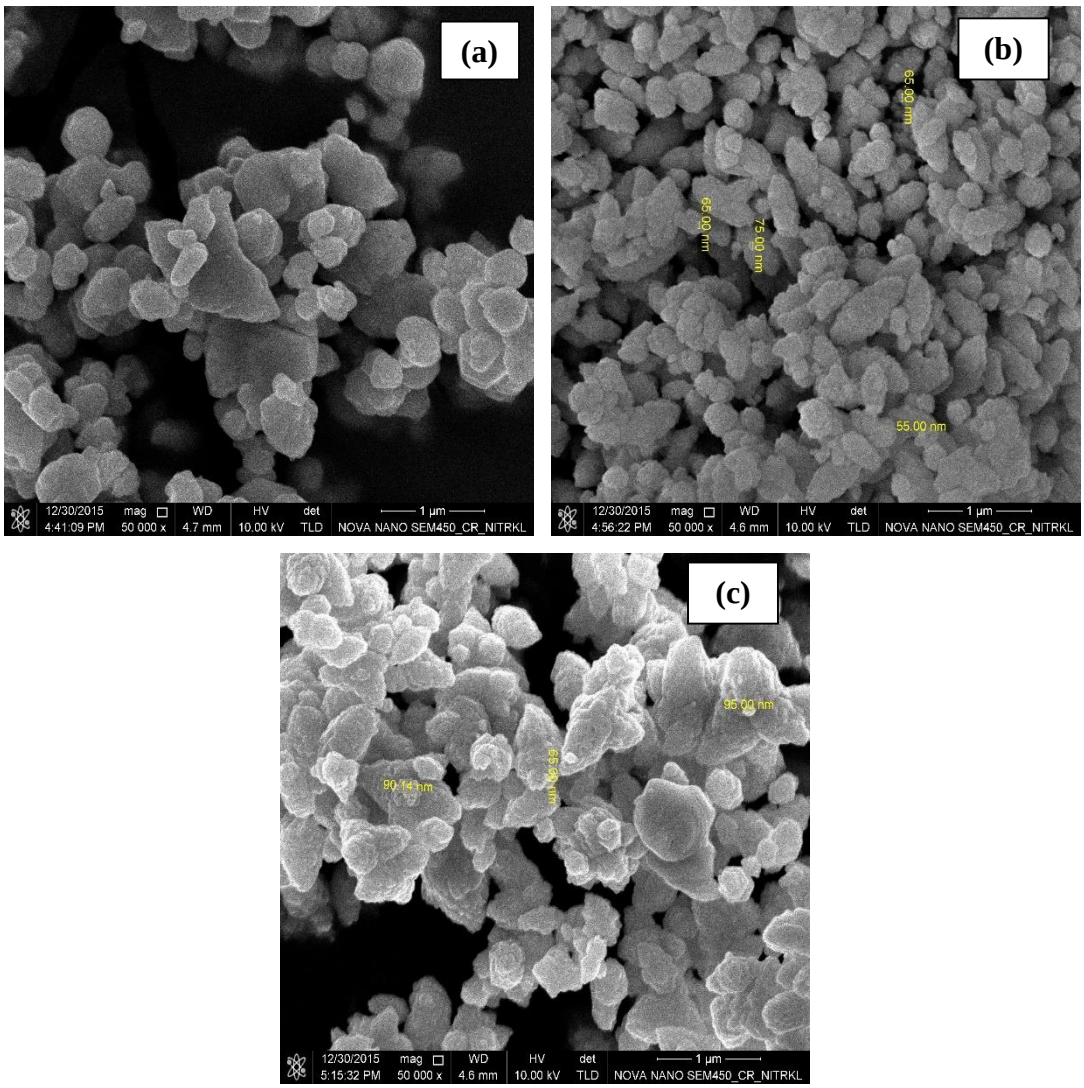

Fig. 4.3: FESEM micrograph of calcined (600 °C) zinc oxide powder prepared using $NaBH_4$ and washed for 10 times (a), 20 times (b) and 30 times (c). Scale bar is 1µm.

Similarly, Fig. 4.4 (a), (b) and (c) shows FESEM micrograph of calcined (800 °C) zinc oxide powder prepared using $NaBH_4$ and washed for 10 times, 20 times and 30 times, respectively. When the powders were washed for 10 times and calcined at 800 °C, the particle size increases when compared with the powders washed for 10 times and calcined at 600 °C. The particles are nearly spherical in nature and also found to be agglomerated. The agglomerated particle size ranges in between 300 nm to 700 nm. However, the powders washed for more than 20 or 30 times, the powder morphology changes to smaller in size, but agglomerated in nature. In the case for washing more than 20 or 30 times, the particle size ranges in between 100 nm to 300 nm. Irrespective of washing time, the particles are found to be nearly spherical in nature after calcination at 800 °C.

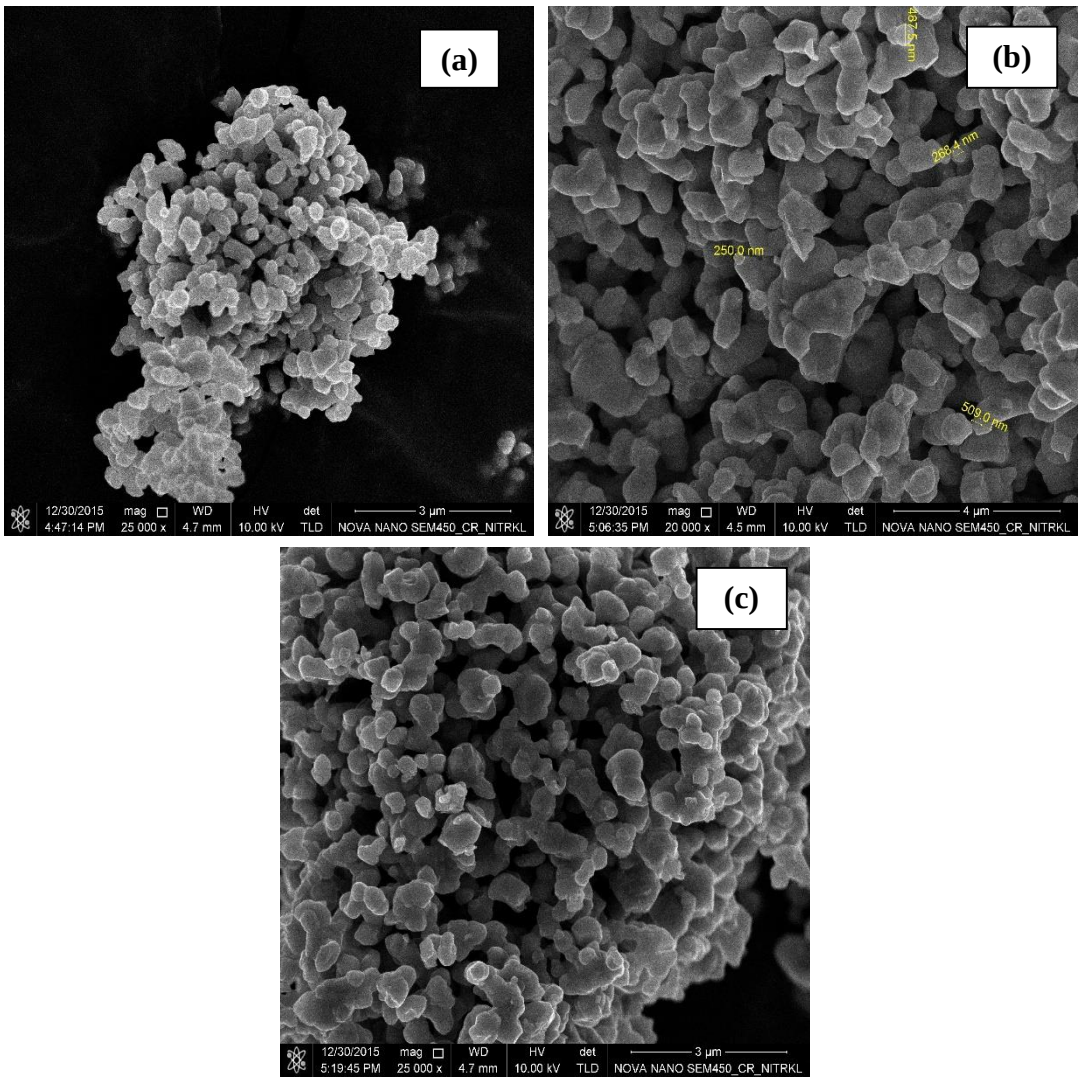

Fig. 4.4: FESEM micrograph of calcined (800 °C) zinc oxide powder prepared using $NaBH_4$ and washed for 10 times (a), 20 times (b) and 30 times (c).

4.4 Remarks

Phase pure zinc oxide was developed via borohydride route using zinc chloride-salt as a precursor and $NaBH_4$ as a precipitating agent. Effect of washing times and calcination temperature on the phase evolution and powder morphology was analyzed. The phase analysis confirmed the formation of impurity zinc-borate phase at higher temperature i.e. 800 °C and at lower number of washings i.e. 10 times. Higher number of washings cause the removal of impurity consists of borate phases and phase pure zinc oxide was formed. So in order to develop phase pure ZnO, it was necessary to wash the precipitated sample for at least 20 number of washings.

Further, phase evolution of zinc-borate phase in zinc oxide matrix may also depend on the zinc-salt precursor. In order to study the effect of zinc-salt precursor on the phase evolution of zinc oxide and zinc-borate, two different samples were prepared using same borohydride method using zinc-chloride and zinc-acetate precursor and washed for the optimized washing time i.e. 20 times. Thermal behavior, phase evolution, powder morphology and UV-vis was studied and discussed in next chapter.

Chapter 5

Effect of precursor and calcination temperature on the phase evolution and powder morphology of zinc oxide and or zinc borate

5.1 Introduction

This chapter deals with the synthesis of zinc oxide powders via borohydride route using $NaBH_4$ using chloride as well as acetate precursor. In addition, the precipitated powders after the reaction were washed for the optimized times i.e. 20 times with hot water. Thermal behaviour was studied for the as-synthesized powders. Further, these washed samples were calcined at 450 °C, 600 °C and 800 °C. Phase evolution was studied using XRD and powder morphology of these powders were analysed using FESEM and absorption study was done using UV-vis spectrometer.

5.2 Thermal Analysis

In order to study the temperature at which amorphous nature of as-synthesized powder converts to crystalline nature, thermal behavior was investigated using DSC-TG. Fig. 5.1 and 5.2

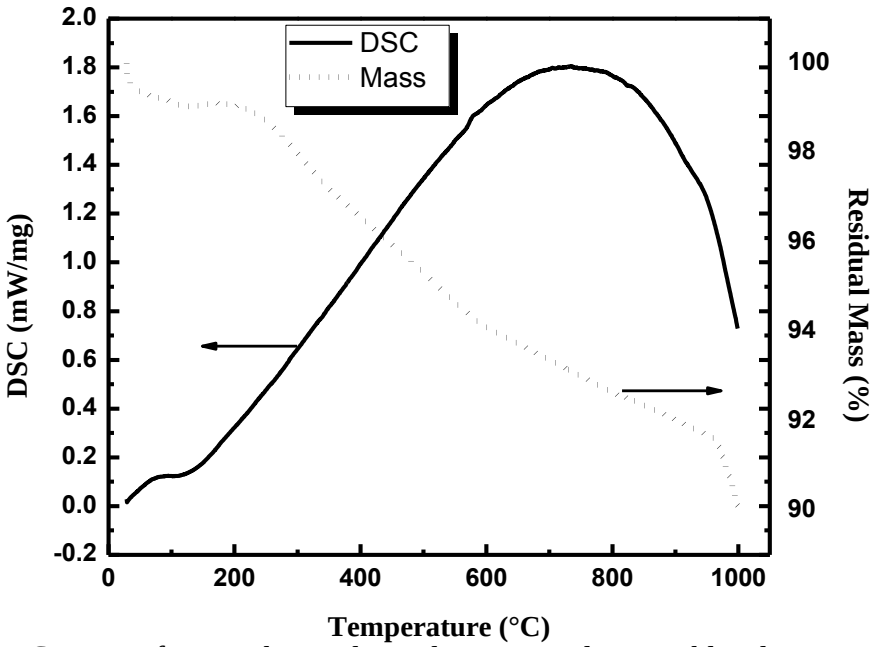

5.1: DSC-TG curve of as-synthesized powder, prepared using chloride precursor.

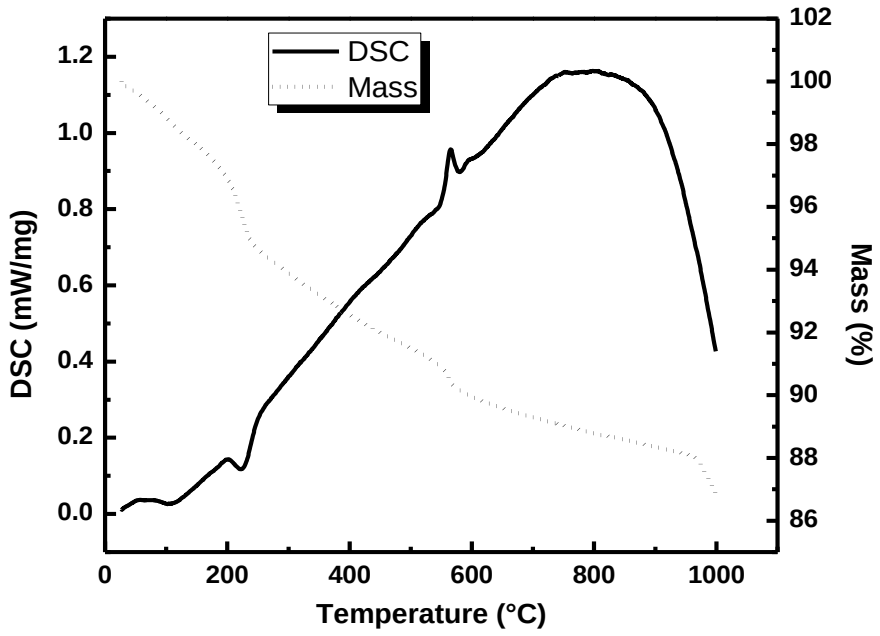

Fig. 5.2: DSC-TG curve of as-synthesized powder, prepared using acetate precursor.

Figure 5.1 shows DSC-TG curve of as-synthesized powder, prepared using chloride precursor. Similarly, DSC-TG curve of as-synthesized powder, prepared using acetate precursor was shown in Fig. 5.2. Both as-synthesized samples show similar trend in DSC-

TG curve. However, a total weight loss of around 10 % and 14 % was observed in the temperature range from room temperature to 1000 °C for the case of chloride precursor and acetate precursor, respectively. Comparing DSC curve of both sample, the endothermic peak in the range of 100 °C to 250 °C corresponds to evaporation of adsorbed water and this led to decrease in mass of about 3 % in both samples, based on the TG curve. There was a broad peak starting from 400 °C to 1000 °C with a maximum peak at around 800 °C. In addition, a sharp peak was observed at around 600 °C for the sample prepared using acetate precursor. This peak was very minute in case for the sample prepared using chloride precursor. This broad peak along with a sharp peak may corresponds to the crystallization behaviour of the as-synthesized powder. To further confirm the crystallization behaviour of the as-synthesized powder, these powders were calcined at 450 °C, 600 °C and 800 °C. Phase analysis was performed on these calcined powder using XRD.

5.3 Phase analysis

Figure 5.3 indicates the XRD patterns of calcined (at three different temperatures) powders, prepared using chloride precursor. All the XRD peaks of calcined powders were matched with phase pure ZnO, as per JCPDS file number 79-0206. All the peaks are indexed with (h k l) values in the XRD patterns. The crystallite size of ZnO, calcined at different temperatures was determined using Scherrer's formula and given in Table 5.1. As seen from the Table 5.1, it was confirmed that the crystallite size increases with calcination temperatures. However, the crystallite size ranges in between 15 nm to 31 nm within this temperature range. Similarly, XRD patterns of calcined (at three different temperatures) powders, prepared using acetate precursor was shown in Fig. 5.4. In this case, phase pure ZnO was formed when the sample calcined at 450 °C, whereas, a minute amount of zinc borate ($Zn_3(BO_3)_2$) was developed in the ZnO matrix when the sample was calcined at 600°C. This zinc borate phase was prominent when the sample was calcined at 800 °C. The crystallite size of ZnO was determined using Scherrer's formula and given in Table 5.2. As seen from the Table 5.2, it was confirmed that the crystallite size slightly increases with calcination temperatures. In this case, the crystallite size ranges in between 17 nm to 35 nm within this temperature range.

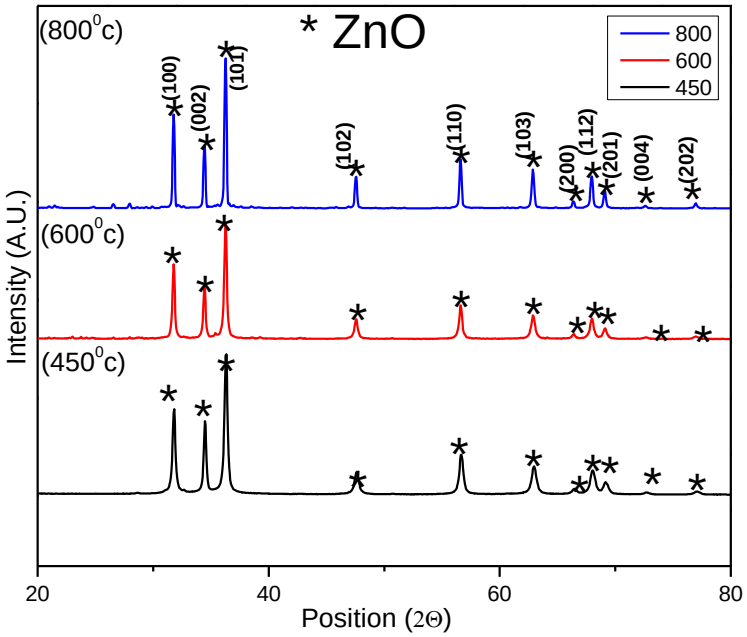

Fig.5.3: XRD patterns of calcined powders, prepared using chloride precursor.

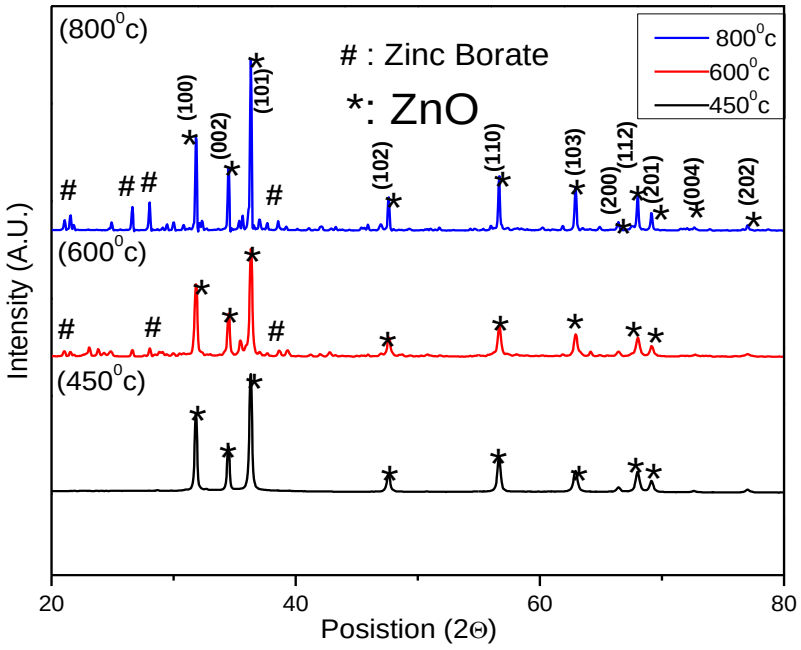

Fig. 5.4: XRD patterns of calcined powders, prepared using acetate precursor.

Table 5.1: Crystallite size of ZnO, prepared using chloride precursor.

Calcined at 450 °C				
Peak Number	Peak Position (2θ) (in degree)	β(FWHM) (radians)	Crystallite size (nm)	Average Crystallite Size (nm)
1	31.8073	0.0101	14.2	15
2	34.4929	0.0087	16.6	
3	36.3077	0.0104	14.1	
Calcined at 600 °C				
Peak Number	Peak Position (2θ) (in degree)	β(FWHM) (radians)	Crystallite size (nm)	Average Crystallite Size (nm)
1	31.8032	0.0079	18.1	18
2	34.4685	0.0080	17.9	
3	36.2958	0.0087	16.7	
Calcined at 800 °C				
Peak Number	Peak Position (2θ)(in degree)	β(FWHM) (radians)	Crystallite size (nm)	Average Crystallite Size (nm)
1	31.8016	0.0113	12.6	31
2	34.4658	0.0036	39.6	
3	36.2919	0.0035	40.9	

Table 5.2: Crystallite size of ZnO, prepared using acetate precursor.

Calcined at 450 °C				
Peak Number	Peak Position (2θ) (in degree)	β(FWHM) (radians)	Crystallite size (nm)	Average Crystallite Size (nm)
1	31.8550	0.0083	17.2	16
2	34.5133	0.0042	34.2	
3	36.3413	0.0044	32.0	
Calcined at 600 °C				
Peak Number	Peak Position (2θ) (in degree)	β(FWHM) (radians)	Crystallite size (nm)	Average Crystallite Size (nm)
1	31.8685	0.0093	15.5	17
2	34.5370	0.0081	17.7	
3	36.3691	0.0086	16.9	
Calcined at 800 °C				
Peak Number	Peak Position (2θ)(in degree)	β(FWHM) (radians)	Crystallite size (nm)	Average Crystallite Size (nm)
1	31.8667	0.0052	27.231	33
2	34.5249	0.0052	31.621	
3	36.3550	0.0052	37.818	

5.4 Powder morphology

Further powder morphology of ZnO powders prepared using chloride and acetate precursor was studied using FESEM. Fig. 5.5 and Fig. 5.6 show the FESEM micrographs of calcined ZnO powders, prepared by chloride and acetate precursor, respectively. It was observed that the particles of ZnO were agglomerated in nature when the sample was prepared by chloride process and calcined at 450 °C. In this case, ultra-fine particles are coagulated and form an agglomerated particles. The agglomerated particles are in the range between 100 nm to 500 nm.

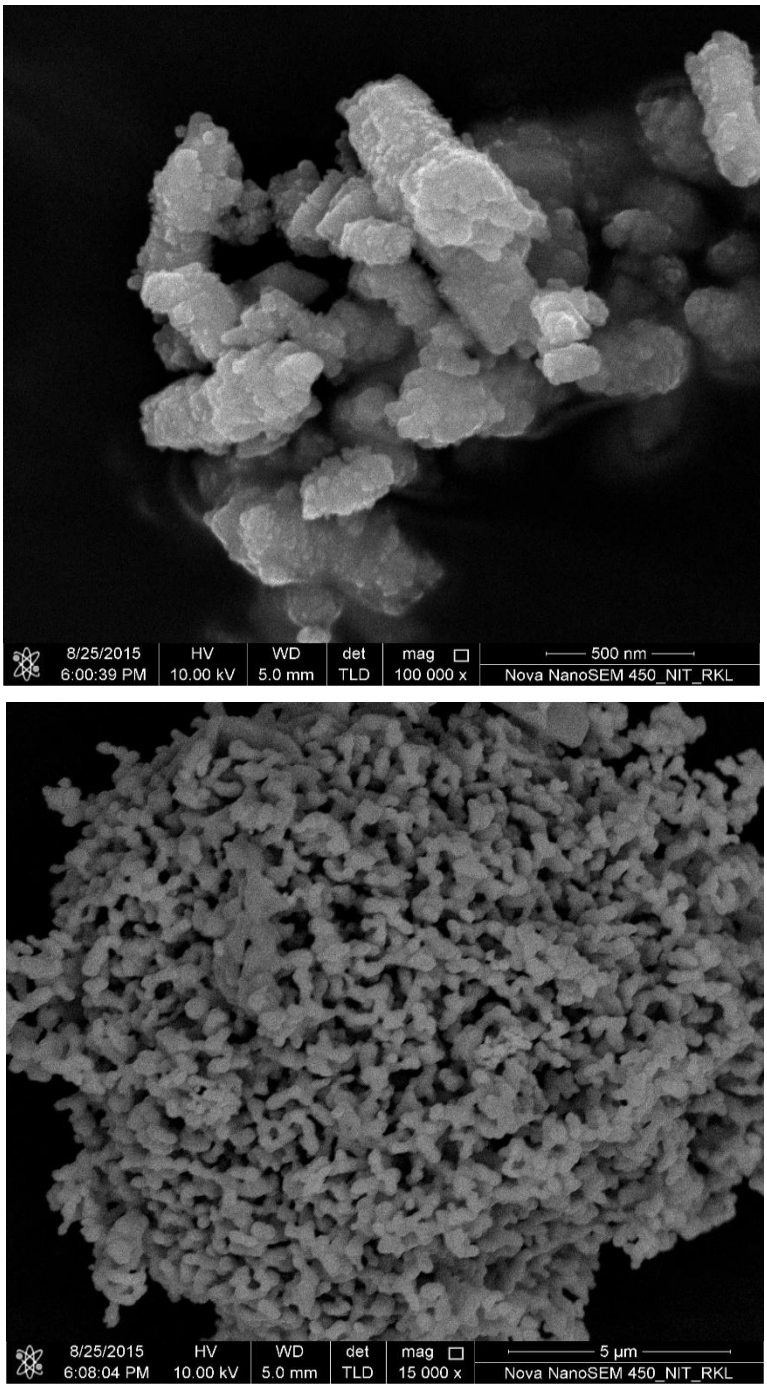

Fig. 5.5: FESEM images of calcined ZnO powders, prepared by chloride precursor.

However, the particles are bigger in size when the sample was prepared using acetate precursor and calcined at the same temperature, i.e., 450 °C. In this case, the particles are less agglomerated in nature and the particles are nearly spherical in nature. The particles are in the range between 50 nm to 300 nm.

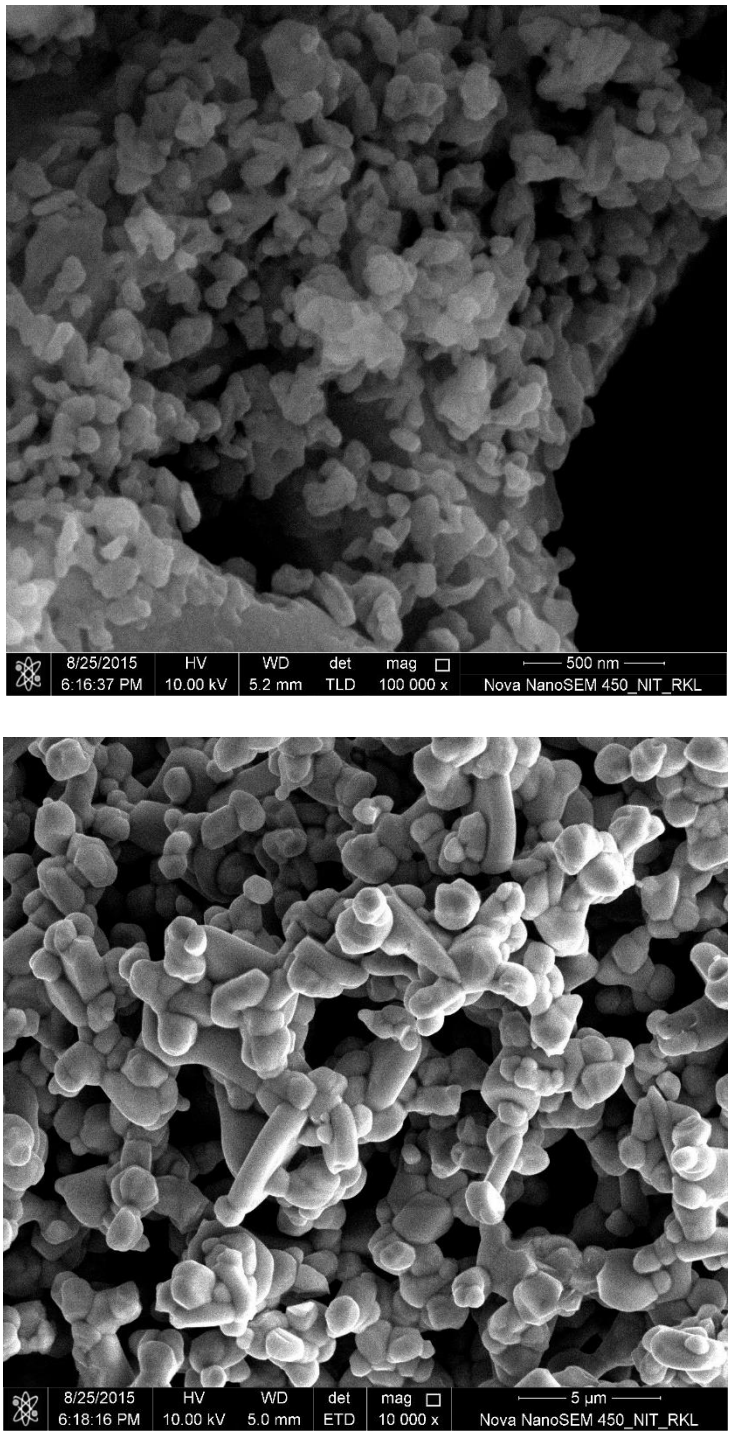

Fig. 5.6: FESEM images of calcined ZnO powders, prepared by acetate precursor.

When the sample was heated at 800 °C, the powder morphology of both the sample was quite similar, but the particle size was different. As seen from Fig. 5.5 and Fig. 5.6, it was observed that the particle size was much smaller in case for the sample prepared using chloride precursor and the particles are much agglomerated with bigger in size for the sample prepared using acetate process. The bigger size of particles for acetate precursor

process may be due to the presence of borate phase. The borate phase may play a role for increasing the particle size during calcination process.

5.5 UV-Visible spectroscopy

The room temperature UV-Vis absorption spectra were measured for all samples in the wavelength range of 200 – 800 nm. Fig. 5.7 and Fig. 5.8 indicates the UV-Vis absorption spectra of ZnO powder calcined at different temperatures and prepared using chloride and acetate precursor, respectively. The two plots in Fig. 5.7 and Fig. 5.8 looks similar in nature. The absorbance peak of the powders prepared using chloride precursor and calcined at 450, 600 and 800 was found to be maximum at 379nm, 384nm, 389nm respectively. However, the absorption peak of the powder prepared using acetate precursor and calcined at 450 °C, 600 °C and 800 °C are found to be at 369nm, 378nm, 386nm respectively. This absorption in the range of 380-395 nm is attributed due to the intrinsic band gap absorption of ZnO due to the electron transition from band gap to the conduction band (O_{2p}-> Zn_{3d}).

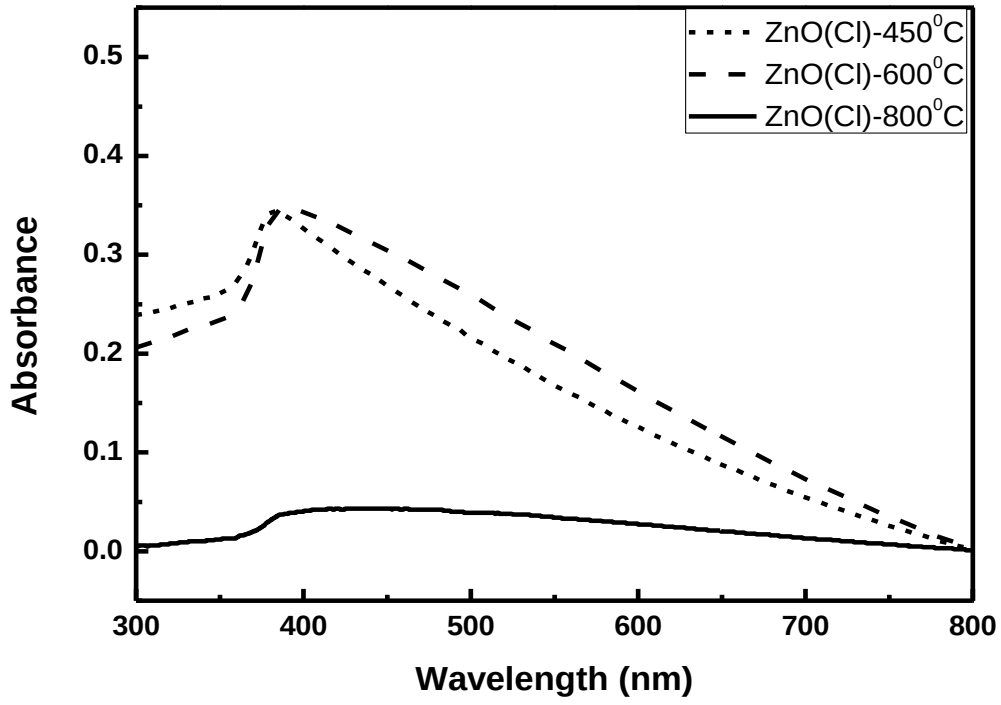

Fig.5.7: UV-Vis spectroscopy curve of ZnO prepared from chloride precursor.

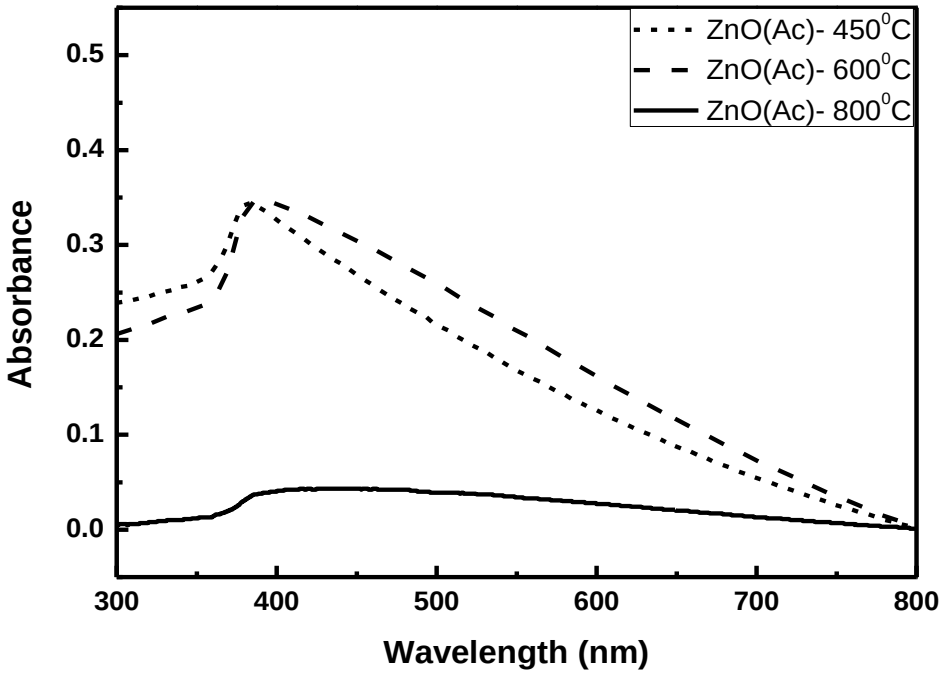

Fig.5.8: UV-Vis spectroscopy curve of ZnO prepared from acetate precursor.

5.6 Summary

Borohydride derived zinc oxide using chloride and acetate precursor was successfully prepared. XRD results revealed that phase pure zinc oxide was formed on the sample prepared using chloride precursor. However, zinc-borate phase was developed at higher temperature when the sample was prepared using acetate precursor. The particle size was smaller in the case of the sample prepared using chloride precursor than the sample prepared using acetate precursor. The absorption in the range of 380-395 nm was attributed due to the intrinsic band gap absorption of zinc oxide. Further, photoluminescence behaviour was studied for Eu^{3+}-doped zinc oxide and Eu^{3+}-doped zinc oxide-zinc-borate sample.

Chapter 6

Photoluminescence behavior of Eu^{3+}-doped zinc oxide and Eu^{3+}-doped zinc oxide-zinc-borate powders.

6.1 Introduction

This chapter deals with the synthesis of Eu^{3+}-doped zinc oxide and Eu^{3+}-doped zinc oxide-zinc-borate powders via borohydride route using $NaBH_4$ using chloride as well as acetate precursor. In addition, the precipitated powders after the reaction were washed for the optimized times i.e. 20 times with hot water. Further, these washed samples were calcined at 600 °C and 800 °C. Phase evolution was studied using XRD and powder morphology of these powders were analyzed using FESEM and photoluminescence behavior was studied using photoluminescence spectroscopy and fluorescence images.

6.2 Phase analysis

Here the Fig. 6.1 and Fig.6.2 shows the phase analysis of the powder prepared by chloride precursor and calcined at 600^0C and 800^0C. It shows the ZnO as the major phase with low intense peaks observed for Zinc Borate ($Zn_3(BO_3)_2$) with JCPDS file number 27-0983 as impurity only in the case of 800^0C sample but no borate phases formed for the 600^0 C calcined sample. The phase evolution of borate phase is enhanced in the 800 ^{o}C calcined sample. Table 6.1 shows the crystallite sizes measured by Scherrer's formula. Here the sizes of 600 ^{o}C & 800 ^{o}C calcined sample are found to be 12nm and 14nm. The peak positions of the major phase of ZnO has shifted towards higher Bragg's angle (2θ) than the undoped ZnO. This peak shifting along with lowering in crystallite size confirms the presence of Eu ion inside the matrix. This doped ions causes lattice distortion due to size difference resulting smaller crystallites. The same pattern is also observed in case of sample prepared through the acetate route. Fig. 6.3 and Fig. 6.4 shows the phase analysis of Europium ion doped zinc oxide prepared by acetate precursor and calcined at 600 ^{o} C & 800^o C respectively. The 600 ^{o}C calcined sample produces pure phase of ZnO whereas the 800 ^{o}C calcined confirms the presence of Zinc Borate ($Zn_3(BO_3)_2$) inside the Zinc Oxide matrix and the peaks are little intense than the chloride route as well confirming the presence of higher amount of zinc borate in case of acetate route. The table 6.2 shows the crystallite size of Eu-doped ZnO prepared acetate precursor and calcined at 600 ^{o}C & 800^{o}C respectively. The sizes were calculated to be 12nm and 14nm for 600 ^{o}C & 800^{o}C respectively.

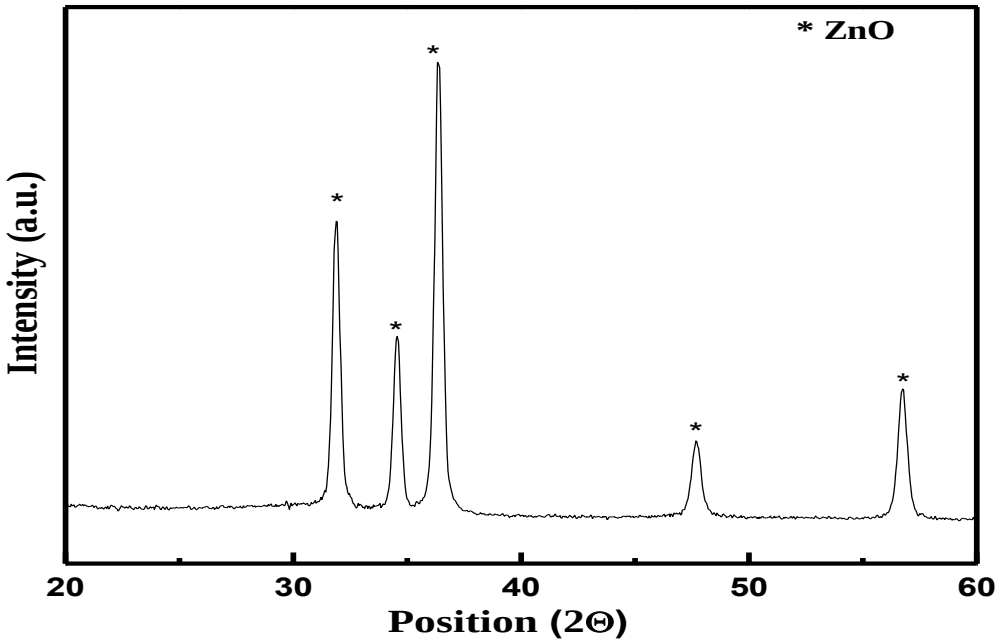

Fig. 6.1:XRD patterns of calcined (600°C) Eu-doped ZnO prepared by chloride route.

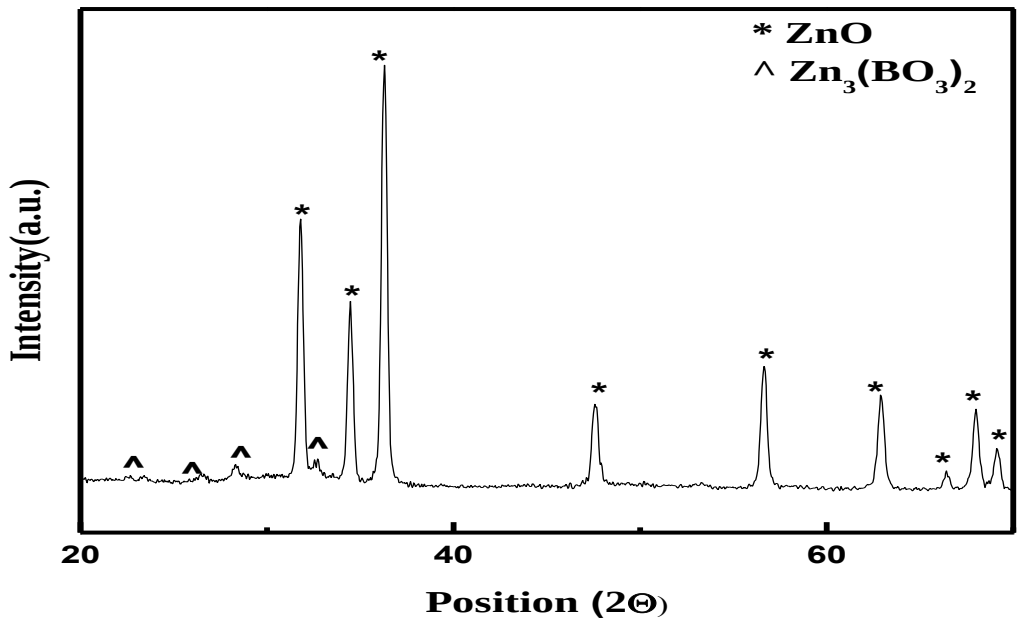

Fig. 6.2:XRD patterns of calcined (800°C) Eu-doped ZnO prepared by chloride route.

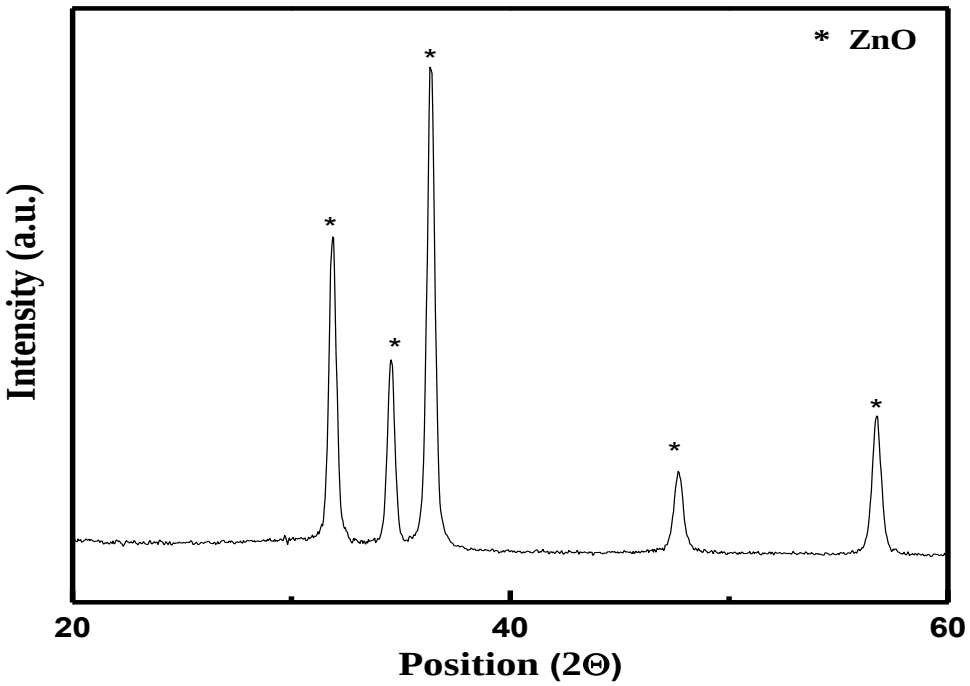

Fig. 6.3:XRD patterns of calcined (600°C) Eu-doped ZnO prepared by acetate route.

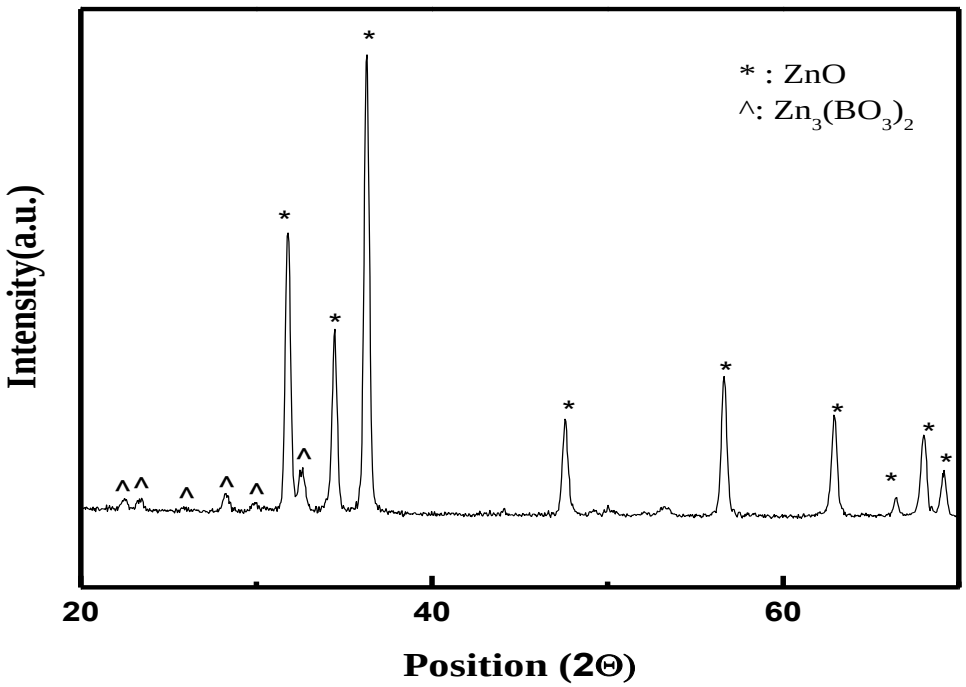

Fig. 6.4: XRD patterns of calcined (800°C) Eu-doped ZnO prepared by acetate route..

Table 6.1: Crystallite size of Eu^{3+}-doped ZnO, prepared using chloride precursor.

Calcined at 600 °C				
Peak Number	Peak Position (2θ) (in degree)	β(FWHM) (radians)	Crystallite size (nm)	Average Crystallite Size (nm)
1	31.848	0.013684	11.92656	12
2	34.498	0.013894	12.10734	
3	36.3935	0.014002	12.29999	
Calcined at 800 °C				
1	31.833	0.012215	13.35899	14
2	34.398	0.012089	13.89771	
3	36.2745	0.012383	13.88733	

Table 6.2: Crystallite size of Eu^{3+}-doped ZnO, prepared using acetate precursor.

Calcined at 600 °C				
Peak Number	Peak Position (2θ) (in degree)	β(FWHM) (radians)	Crystallite size (nm)	Average Crystallite Size (nm)
1	31.83985	0.013691	11.9	12
2	34.53155	0.013576	12.3	
3	36.3725	0.014093	12.2	
Calcined at 800 °C				
1	31.8125	0.012229	13.3	14
2	34.35435	0.011475	14.6	
3	36.334	0.012075	14.2	

6.3 Powder morphology

Further powder morphology of Eu-doped ZnO powders prepared using chloride and acetate precursor and calcined at 600 ^{o}C and 800 ^{o}C were studied using FESEM. Fig. 6.5

and Fig. 6.6 respectively. It was observed in Fig. 6.5 the particles of ZnO were very fine which were in an agglomerated form. The particle size of the fine particles ranged from 30nm to 100nm. However, in case of the 800 ^{o}C calcined sample the particles moreover showed small plates shaped particles which were in the size range of 100 nm to 300 nm.

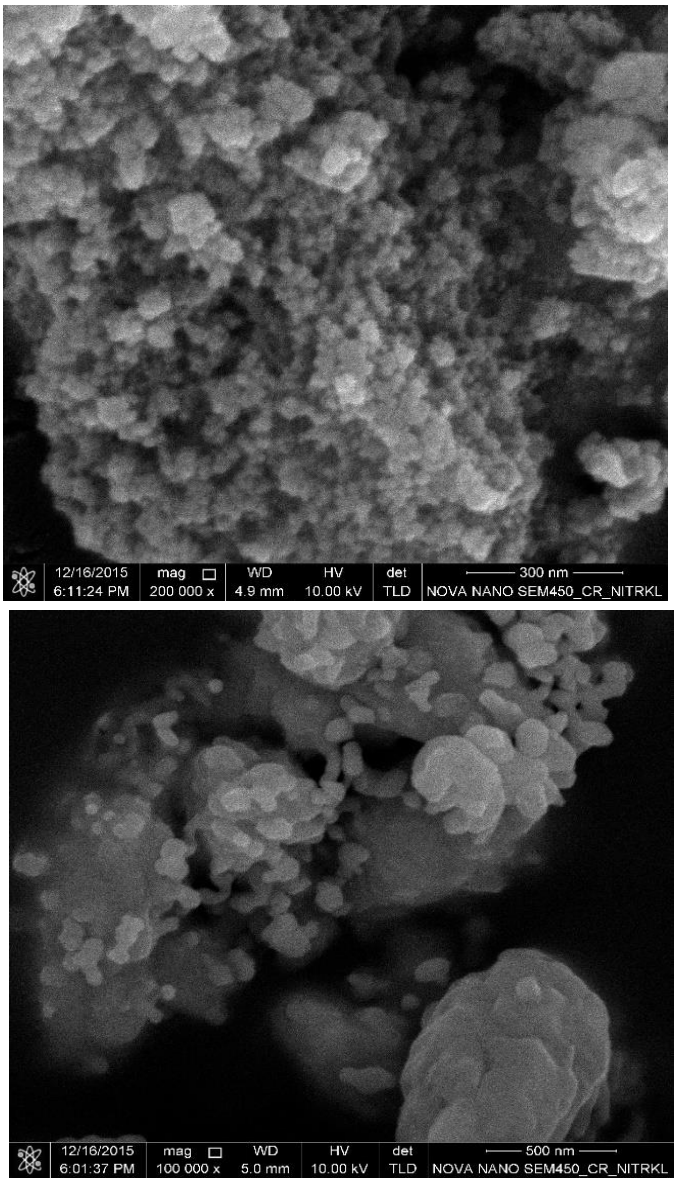

Fig. 6.5: FESEM images of calcined Eu-doped ZnO powders, prepared by chloride precursor.

Considering the Fig. 6.7 where the morphology of Eu-doped ZnO prepared by acetate route and calcined at 600 ^{o}C and 800 ^{o}C , the lower calcined powder morphology is similar to the previous one of chloride precursor but the size of particles are more finer in the range of 30nm to 100nm. But the 800 ^{o}C calcined sample shows nearly spherical particle with uniform distribution of particle with size range 100nm to 500nm.

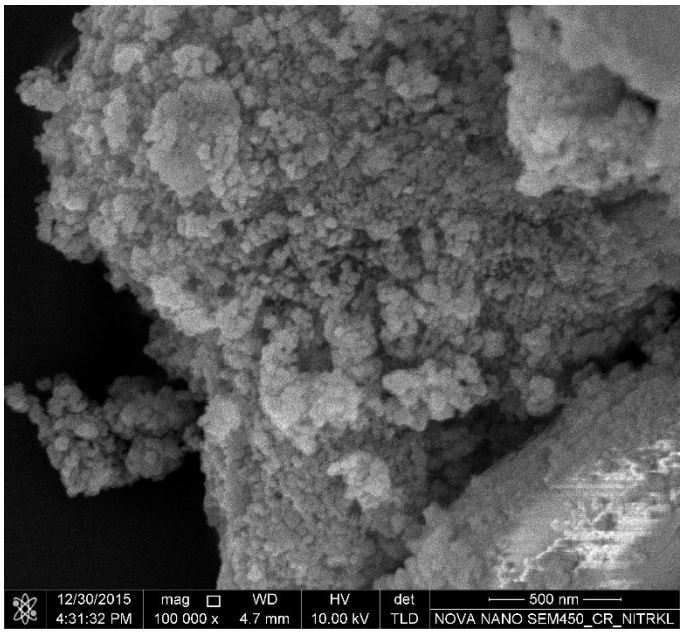

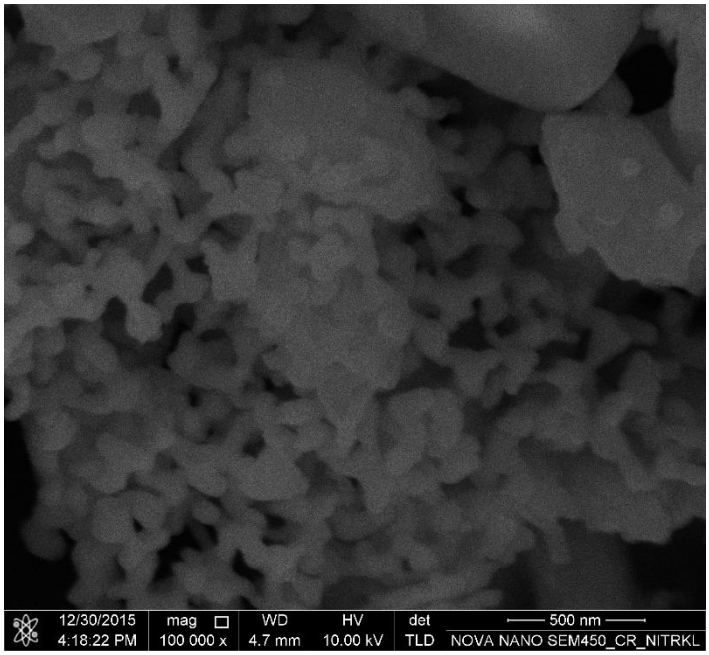

Fig. 6.6: FESEM images of calcined Eu-doped ZnO powders, prepared by acetate precursor.

When the sample was heated at 800 °C, the powder morphology of both the sample was quite similar, but the particle size was different. As seen from Fig. 6.5 and Fig. 6.6, it was observed that the particle size was much smaller in case for the sample prepared using chloride precursor and the particles are much agglomerated with bigger in size for the

sample prepared using acetate process. The bigger size of particles for acetate precursor process may be due to the presence of borate phase. The borate phase may play a role for increasing the particle size during calcination process.

6.4 Photoluminescence

The standard wavelengths in case of a mercury vapor lamp are 254 nm and 365 nm. Hence, these two wavelengths were selected in order to study the response of the prepared samples. The samples were excited at 254 nm and 365 nm, and the properties were compared for the ZnO obtained from chlorides and acetates salts calcined at 600 ^{o} C and 800 ^{o} C.

Considering the chloride salt, the intensity of the samples calcined at 600 ^{o} C and 800 ^{o} C , the intensity of the emission is higher in the case of 254 nm excited samples for both calcined samples. Looking for the effect of calcination temperature, comparing both the graphs for the excitation at 365nm in Fig 6.7(a) and 6.7(b), it is observed that the 800 ^{o} C calcined samples produced excitation peaks at the exact position as that of the 600^{o} C and the pattern of the graph was also same in both the cases. But the peak intensities were higher in the case of 800^{o} C calcined sample compared to the other one. This may be caused due to the presence of the Zinc Borate phase which is evolved during high temperature calcination. However the difference in peak intensities gradually decreases for higher wavelength excitation. When we compared both the graphs for 365nm excited wavelength, many peaks were diminished for the 600 ^{o} C sample as compared to the otherone.

This intensity difference can be seen in the fluorescence microscopy images where at 254 nm excitation wavelength the sample is darker in shade as compared to 365 nm excitation wavelength in case of 600 C sample. Moreover, for the 600 C calcined sample, due to enhanced contribution of the red portion of the emission spectrum, the sample appears to bear a reddish brown hue. Similarly, for 800 C sample, there is a greenish hue due to lesser contribution of the red portion of the emission spectrum. .

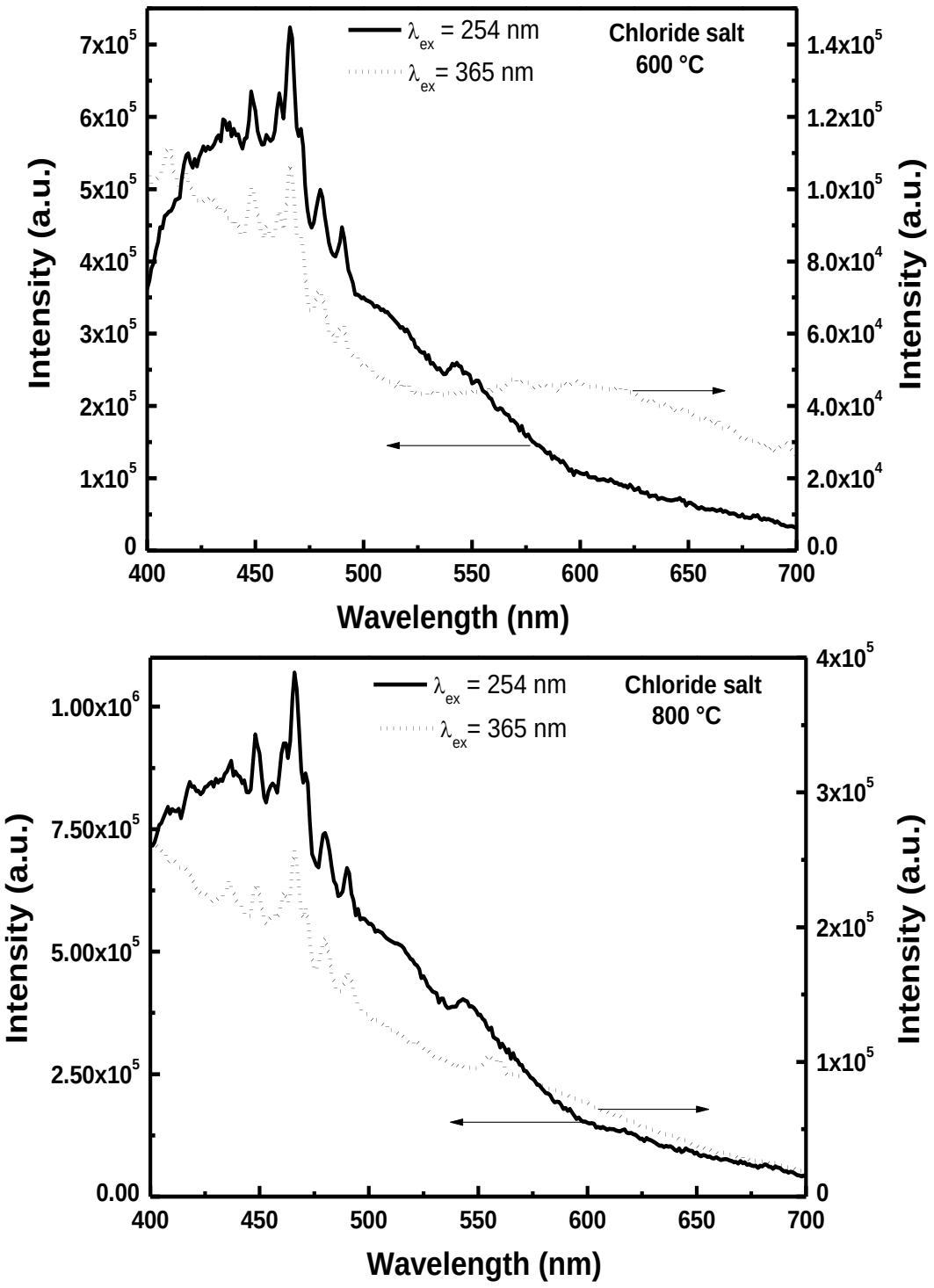

Fig. 6.7: Photoluminescence behavior of the borohydride derived powder (Eu-doped ZnO) prepared by chloride route and excited at 254nm and 365nm.

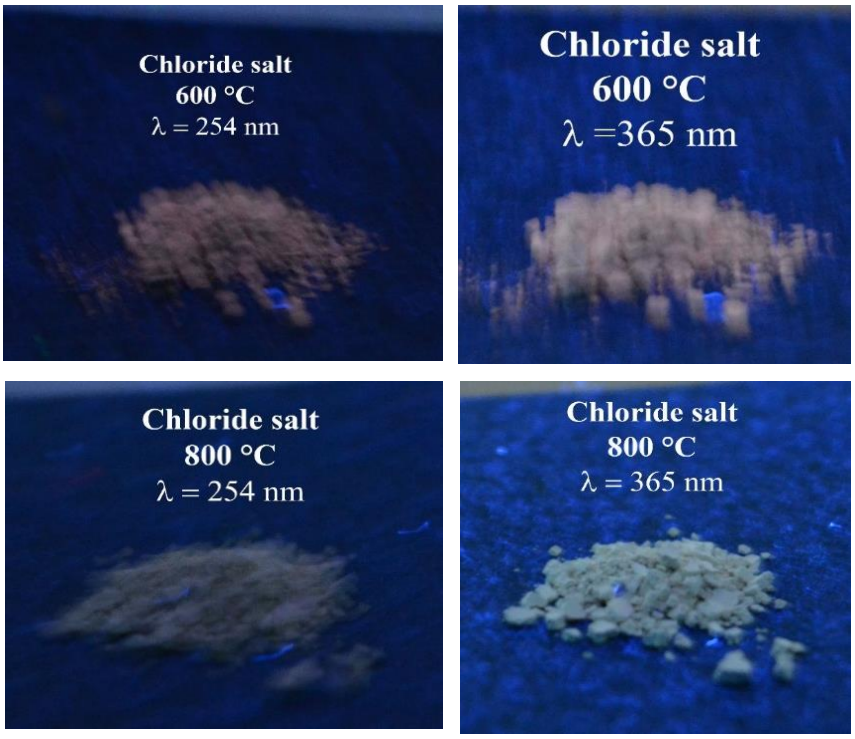

Fig. 6.8: Fluorescence image of the borohydride derived powder under UV lamp (Eu-doped ZnO prepared by chloride route)

For the analysis of ZnO powder prepared using the acetate route, the samples calcined at 600 ^{o} C and 800 ^{o} C were irradiated with the standard wavelengths. It was seen that the intensity of the emission is higher for 800 C calcined samples as compared to 600 C calcined sample for both 254 nm and 365 nm irradiation.The increased intensity in case of 800 ^{o} C sample could be attributed to the evolution of more prominent zinc borate($Zn_3(BO_3)_2$) phase. This zinc borate phase might be the reason for the increased intensity as observed in the 800 ^{o} C sample. The intensity difference of 254 nm and 365 nm for 600 ^{o} C and 800 ^{o} C samples can be seen from the fluorescence microscopy images where at 254 nm excitation wavelength the sample is darker in the shade as compared to 365 nm excitation wavelength. Moreover, for the 600 ^{o} C calcined sample, due to enhanced contribution of the red portion of the emission spectrum, the sample appears to bear a reddish brown hue. Similarly, for 800 C sample, there is a greenish hue due to the lesser contribution of the red portion of the emission spectrum. Moreover, the peak intensities were higher in the case of 800^{o} C calcined sample obtained by acetate route as compared to 800 C calcined sample obtained by the chloride salt. This may be caused due to the presence of the Zinc Borate phase which is evolved and plays a much greater role during high-temperature calcination in the acetate salt. Since the intensity was higher for the samples

obtained by the acetate salt, these samples were used for further analysis of the photoluminescence properties. It has been discussed previously that the absorbance value was higher for a wavelength of 390 nm. Since, the excitation spectrum is closely similar to the absorption spectrum, the 600C and 800 C samples obtained by the acetate salt were irradiated by an excitation wavelength of 390 nm.

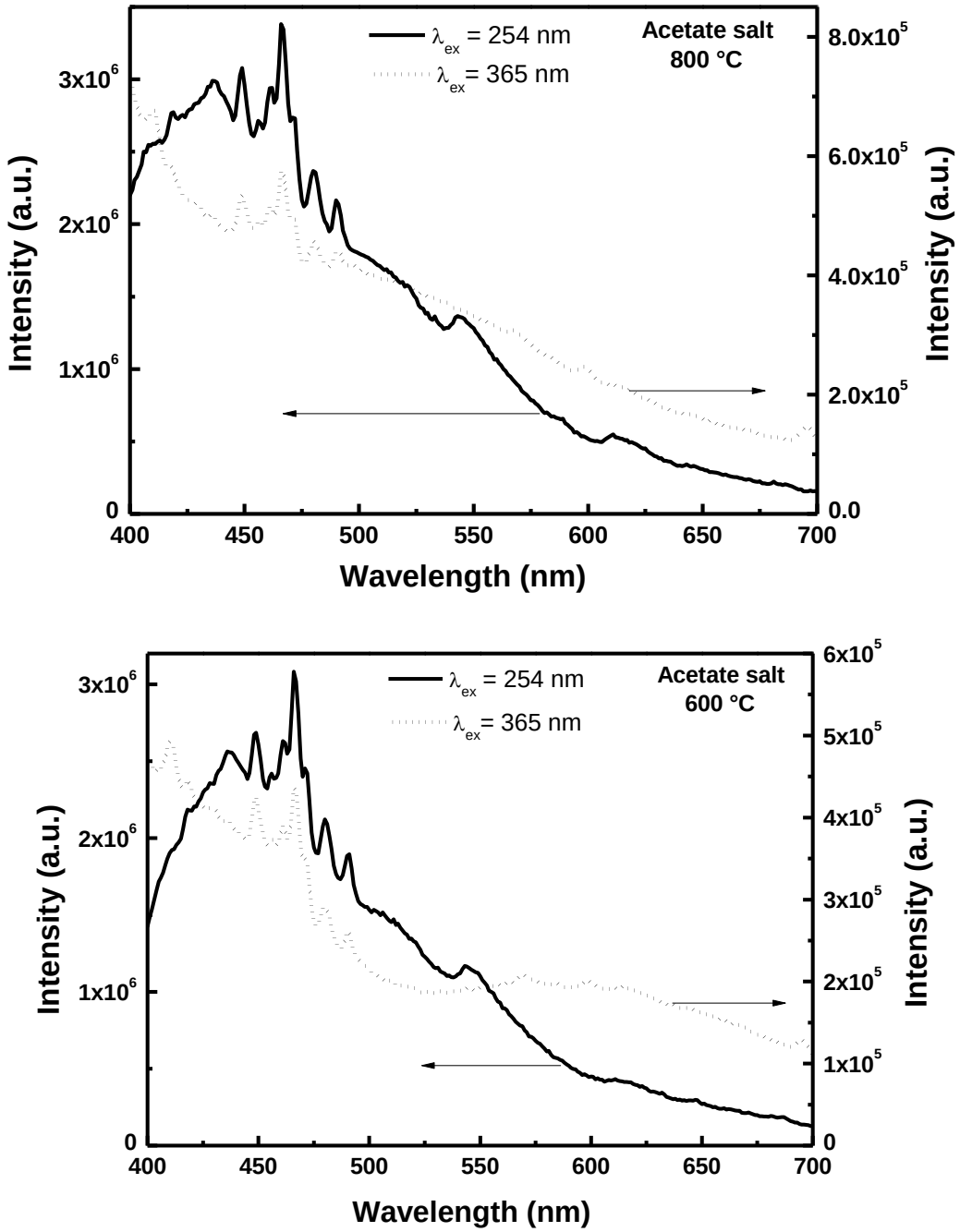

Fig. 6.9: Photoluminescence behavior of the borohydride derived powder (Eu-doped ZnO) prepared by acetate route and excited at 254nm and 365nm.

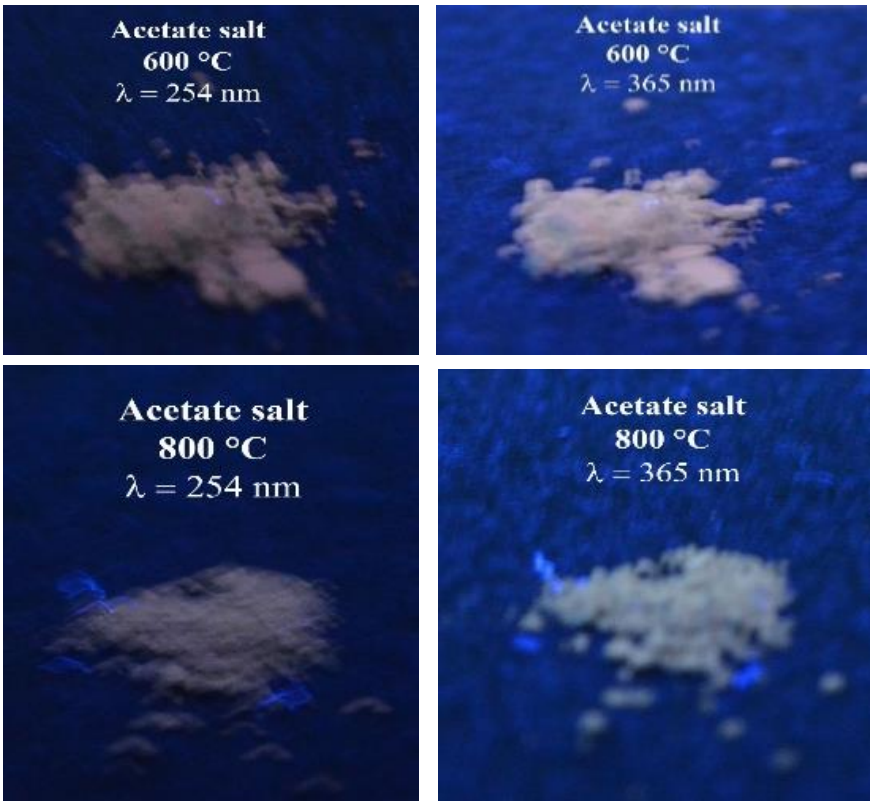

Fig. 6.10: Fluorescence image of the borohydride derived powder under UV lamp (Eu-doped ZnO prepared by acetate route).

As seen from the figure 6.11, we observe the PL curve of Europium doped zinc oxide-zinc borate system calcined at 600 ^{o}C and 800 ^{o}C excited at a wavelength of 390 nm observed in the range of 500nm to 700nm. This excitation wavelength (390nm) corresponds to the absorption peak studied from the UV-vis emission study. We can clearly observe in both the curves showing peaks in green and red region at the positions 531nm, 573nm, 612nm and 640nm. Here the intense peak at the position of 530nm is in the green region produced due to the intrinsic defects of the ZnO crystal (produced by oxygen deficiency). But the later peaks in the higher wavelength region are observed due to the presence of Eu^{+3} ion inside the ZnO crystal. The peaks at 573nm, 612nm and 640nm are due to the transitions taking place for $^{5}D_0 \rightarrow {}^{7}F_{0,}$ $^{5}D_0 \rightarrow {}^{7}F_2$ and $^{5}D_0 \rightarrow {}^{7}F_4$. These peaks confirms the presence of Europium ion and the peaks make it an efficient luminescent material. But comparing both of the PL curves of Eu-doped ZnO prepared by acetate route and calcined at 600 ^{o} C and 800 ^{o}C we can clearly observe the difference between the luminescence of both samples. Though the peak are in same position in both the cases but the peak intensities varied by a huge difference. The 800 ^{o}C calcined sample was observed to show the higher intense peaks

than 600 ^{o} C calcined sample. This may happen due to the formation of higher amount of zinc-borate phase in the higher degree calcined sample. This shows the positive contribution of the borate phase towards the contribution of luminescence.

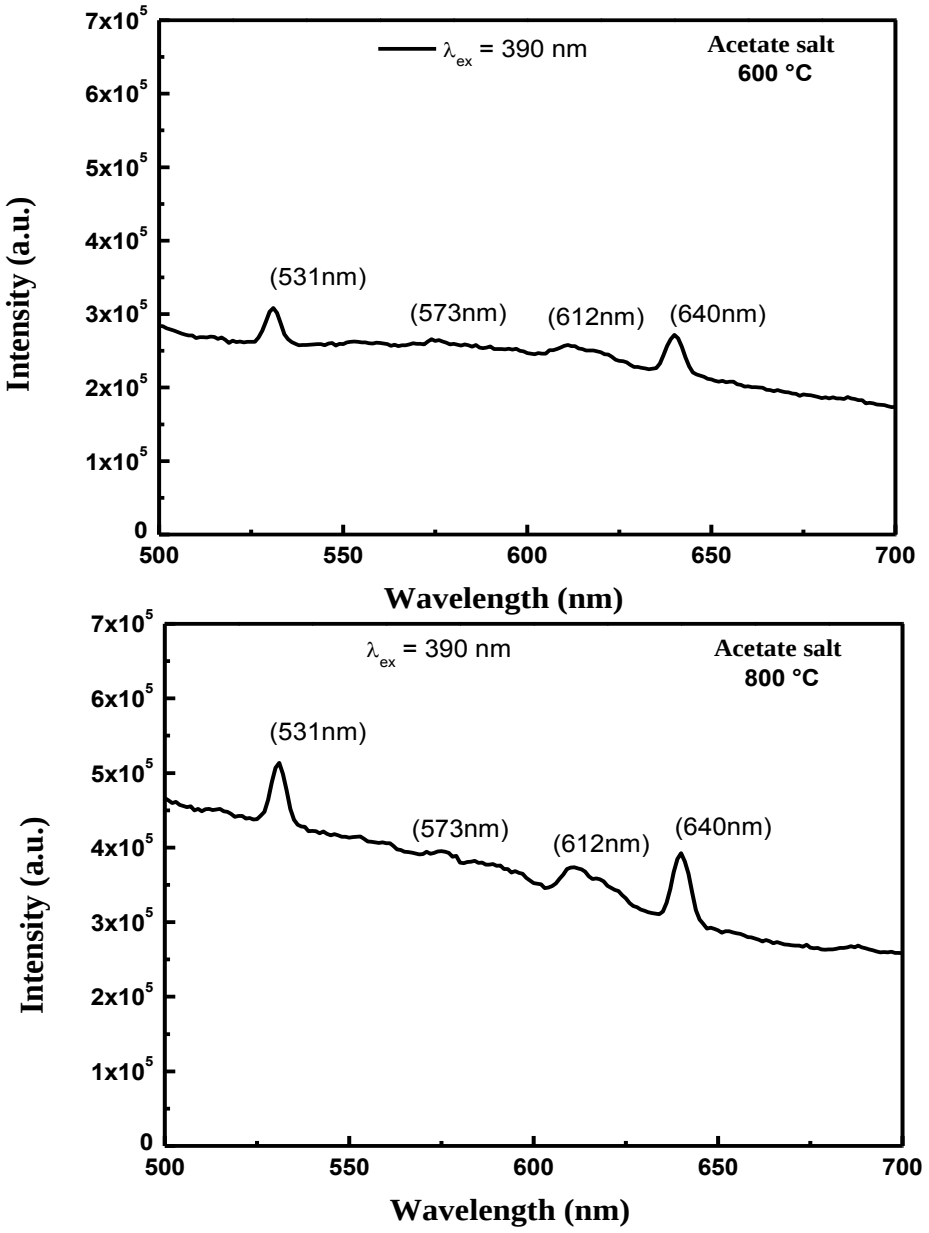

Fig. 6.11: Photoluminescence behavior of the borohydride derived powder (Eu-doped ZnO) prepared by acetate route and excited at 390nm

Chapter 7

CONCLUSIONS

Based on the results and discussion, the following points are the main findings of this project work.

- Though the sodium borohydride is a strong reducing agent for preparing metal nanoparticles, it also acts as a precipitating agent to form oxide powders.
- Using sodium borohydride, zinc oxide and mixture of zinc oxide and zinc-borate powders were successfully prepared.
- The number of washings and calcination temperature have significant effects in producing pure phase of zinc oxide.
- The amount of zinc-borate strongly depends on the zinc-salt precursor as well as calcination temperature.
- The chloride route is preferred over acetate precursor as it produces phase pure ZnO with finer particle size.
- The particle size was found to be in the range between 50 nm to 300 nm when the sample was prepared using chloride precursor.
- The particles were finer in size and agglomerated in nature when calcined at lower temperature and forms nearly spherical in nature when calcined up to 800 °C, irrespective of the precursor.
- When Eu^{3+} was doped during preparing zinc oxide powder, it was found that phase pure zinc oxide was formed at 600 °C, and zinc-borate phase was suppressed at 800 °C.
- However, the amount of zinc borate (when calcined at 800 °C) was lower in the case of the sample prepared using chloride precursor when compared with the sample prepared using acetate precursor.
- The photoluminescence intensity (when excited at 254 nm, 365 nm and 390 nm) was found to be higher in case of the sample prepared using acetate precursor as compared to the chloride precursor sample. This could be attributed to the presence of a higher quantity of zinc-borate phase in the zinc oxide matrix.

The present observation and discussion suggest that the borohydride derived Eu^{3+}-doped zinc oxide, and Eu^{3+}-doped zinc oxide-zinc-borate may be a strong candidate for phosphor application.

References

1. T. Aoki, "Photoluminescence Spectroscopy," *Charact. Mater.*, 2002 , **3**, 1-7.
2. R. Ye and A. R. Barron, "Photoluminescence Spectroscopy and its Applications", 2012, 1–10.
3. S. Singh, P. Thiyagarajan, K. M. Kant, D. Anita, S. Thirupathiah, N. Rama, B. Tiwari, M. Kottaisamy, M. S. R. Rao, K. Mohan Kant, D. Anita, S. Thirupathiah, N. Rama, B. Tiwari, M. Kottaisamy, and M. S. Ramachandra Rao, "Structure, microstructure and physical properties of ZnO based materials in various forms: bulk, thin film and nano," *J. Phys. D. Appl. Phys.*, 2007, **40**, 6312–6327,
4. C. F. Klingshirn, "ZnO: Material, physics and applications," *ChemPhysChem*, 2007, **8**, 782–803.
5. M. Vaseem, A. Umar, and Y. Hahn, "ZnO Nanoparticles : Growth, Properties, and Applications", *J. Phys.: Condens. Matter*, 2010, **5,** 829-858..
6. C. Li, G. Fang, N. Liu, J. Li, L. Liao, F. Su, and G. Li, "Structural , Photoluminescence, and Field Emission Properties of Vertically Well-Aligned ZnO Nanorod Arrays Structural , Photoluminescence , and Field Emission Properties of Vertically Well-Aligned", *J. Phys. Chem*, 2007, **111**, 12566–12571.
7. S. K. Mishra, R. K. Srivastava, and S. G. Prakash, "Photoluminescence and photoconductivity studies of ZnO nanoparticles prepared by solid state reaction method," *J. Mater. Sci. Mater. Electron.*, 2012, **24**, 125–134.
8. K. SowriBabu, A. R. Reddy, C. Sujatha, K. V. Reddy, and A. N. Mallika, "Synthesis and optical characterization of porous ZnO," *J. Adv. Ceram.*, 2013,. **2**, 260–265.
9. N. L. Tarwal, P. R. Jadhav, S. A. Vanalakar, S. S. Kalagi, R. C. Pawar, J. S. Shaikh, S. S. Mali, D. S. Dalavi, P. S. Shinde, and P. S. Patil, "Photoluminescence of zinc oxide nanopowder synthesized by a combustion method," *Powder Technol.*, 2011, **208**, 185–188.
10. T. Adschiri, Y. Hakuta, K. Sue, K. Arai. "Hydrothermal Synthesis of Metal Oxide Nanoparticles at Supercritical Conditions" *J. Nanopart. Res.*, 2001, **3**, 227- 235.
11. L. Fan, H. Song, T. Li, L. Yu, Z. Liu, G. Pan, Y. Lei, X. Bai, T. Wang, Z. Zheng, and X." Hydrothermal synthesis and photoluminescent properties of ZnO nanorods", *Journal of Luminescence*, 2007, **122–123**, 819–821.
12. L. Kumari, W. Z. Li, C. H. Vannoy, R. M. Leblanc, and D. Z. Wang, "Zinc oxide micro- and nanoparticles: Synthesis, structure and optical properties," *Mater. Res. Bull.*, 2010, **45**, 190–196.

13. B. Kiliç, E. Gür, and S. Tüzemen, “Nanoporous ZnO photoelectrode for dye-sensitized solar cell,” *J. Nanomater.*, 2012, **2012**, 1-7.
14. P. B. Taunk, R. Das, D. P. Bisen, and R. K. Tamrakar, “Synthesis, structural characterization and study of blue shift in optical properties of zinc oxide nano particles prepared by chemical route method,” *Superlattices Microstruct.*, 2015, **88**, 417–425.
15. S. Shit, T. Kamilya, and P. K. Samanta, “A novel chemical reduction method of growing ZnO nanocrystals and their optical property,” *Mater. Lett.*, 2014, **118**, 123–125,.
16. López-Romero, Sebastián, et al. "Bright Red Luminescence and Structural Properties of Eu 3+ Ion Doped ZnO by Solution Combustion Technique."*World Journal of Condensed Matter Physics*, 2014, **4,** 227.
17. H. V. S. Pessoni, L. J. Q. Maia, and A. Franco, “Eu-doped ZnO nanoparticles prepared by the combustion reaction method: Structural, photoluminescence and dielectric characterization,” *Mater. Sci. Semicond. Process.*, 2015, **30**, 135–141.
18. Ishizumi, Atsushi, Satoshi Fujita, and Hisao Yanagi. "Influence of atmosphere on photoluminescence properties of Eu-doped ZnO nanocrystals." *Optical Materials*, 2011, **33,** 1116-1119.
19. H. Shahroosvand, & M. Ghorbani-asl,.”Solution-based synthetic strategies for Eu doped ZnO nanoparticle with enhanced red photoluminescence”, *Journal of Luminescence*, 2013, **144**, 223-229.
20. S. Srivastava, A. Mondal, N. K. Sahu, S. K. Behera, and B. B. Nayak, “Borohydride synthesis strategy to fabricate YBO3:Eu3+ nanophosphor with improved photoluminescence characteristics,” *RSC Adv.*, 2015, **5**, 11009–11012,.
21. A. Ivankov, J. Seekamp, and W. Bauhofer, “Optical properties of zinc borate glasses,” *Mater. Lett.*, 2001, **49**, 209–213.
22. Y. Zheng, Y. Qu, Y. Tian, C. Rong, Z. Wang, S. Li, X. Chen, and Y. Ma, “Effect of Eu3+-doped on the luminescence properties of zinc borate nanoparticles,” *Colloids Surfaces A Physicochem. Eng. Asp.*, 2009, **349**, 19–22.
23. H. Arrison and I. Ngerson, “Anhydrous Zinc Borate as a Host Crystal in Luminescence *.”,*Z . N a t u r f o r s c h g,* 1961, **16 a** , 920—927.
24. G.J. Janseen, “Information on the FESEM (Field-emission Scanning Electron Microsope) Radbound University Nijema”, 2015.
25. K. N. Shinde, “Phosphate Phosphors for Solid-State Lighting”, *Springer Series in Materials Science*, 2013, **174,** 41-59